HHS Public Access

Author manuscript

Adv Healthc Mater. Author manuscript; available in PMC 2020 March 01.

Published in final edited form as:

Adv Healthc Mater. 2019 March ; 8(6): e1801158. doi:10.1002/adhm.201801158.

Molecular Engineering of Functional Nucleic Acid Nanomaterials toward In Vivo Applications

JingJing Zhang,

Department of Chemistry, University of Illinois at Urbana–Champaign, 601 S. Mathews Ave., Urbana, IL 61801, USA

Tian Lan, and

GlucoSentient, Inc., 2100 S. Oak Street Suite 101, Champaign, IL 61820, USA

Yi Lu

Department of Chemistry, University of Illinois at Urbana–Champaign, 601 S. Mathews Ave., Urbana, IL 61801, USA

Abstract

Recent advances in nanotechnology and engineering have generated many nanomaterials with unique physical and chemical properties. Over the past decade, numerous nanomaterials have been introduced into many research areas, such as sensors for environmental monitoring, food safety, point-of-care diagnostics, and as transducers for solar energy transfer. Meanwhile, functional nucleic acids (FNAs) including nucleic acid enzymes, aptamers, and aptazymes, have attracted great attention from the biomedical community, due to their unique target recognition and catalytic properties. Benefiting from the recent progress of molecular engineering strategies, the physicochemical properties of nanomaterials have been endowed by the target recognition and catalytic activity of FNAs in the presence of a target analyte, resulting in numerous intelligent nanoprobes for diverse applications including intracellular imaging, drug delivery, in vivo imaging, and tumor therapy. This progress report focuses on the recent advances in designing and engineering FNAs-based nanomaterials, highlighting the functional outcomes toward *in vivo* applications. The challenges and opportunities for the future translation of FNAs-based nanomaterials into clinical applications, are also discussed.

Graphical Abstract

This progress report covers recent advances in designing and engineering functional nucleic acids-based nanomaterials, highlights the functional outcomes toward in vivo applications, and discusses the challenges and opportunities for the future translation into clinical applications.

Keywords

functional nucleic acid; DNAzyme; aptamer; nanomaterials; *in vivo* applications

Conflict of Interest

The authors declare no conflict of interest.

1. Introduction

Recent advances in nanotechnology and engineering have generated many nanomaterials with unique physical and chemical properties,[1] such as noble metal nanomaterials with localized surface plasmon resonances, upconversion nanoparticles (UCNPs) with non-linear optical processes, semiconductor quantum dots (QDs) with size-tunable photoluminescence (PL), and carbon nanomaterials with broad absorbance from UV to NIR regions. As a result, much efforts have devoted toward applying these nanomaterials for applications, such as sensors for environmental monitoring, food safety, point-of-care diagnostics, and as transducers for solar energy transfer. An equally exciting and perhaps more challenging field of application is toward their *in vivo* applications, including living animals and human bodies, in diverse areas,[2] such as sensing, drug delivery, medical imaging, and cancer therapy. However, most of these nanomaterials lack selectivity toward targets of interests. Therefore, to employ these nanomaterials for a wider range of *in vivo* applications, various molecular engineering approaches have been employed to obtained nanomaterials functionalized with biomolecules to enable selective targeting.[3–5] Among these biomolecules, Functional Nucleic Acids, or FNAs, have shown the most promise.

FNAs are DNA or RNA molecules that can interact with or bind to a specific analyte, resulting in a conformation change and/or a catalytic reaction.[6] As their names suggested, ribozymes and deoxyribozymes (called DNAzyme hereafter) can act as enzymes in the presence of cofactors to catalyze various chemical reactions, including cleavage and ligation of RNA/DNA, phosphorylation and peroxidation of DNA. On the other hand, riboswitches and DNA aptamers are antibody-like receptors that can bind target molecules with high affinity and selectively. Furthermore, the binding abilities of riboswitches and aptamers can be combined with the enzymatic function of ribozymes and DNAzymes to form aptazymes so that the binding of targets can inhibit or enhance the catalytic activities. These nucleic acids, including DNAzymes, aptamers, and aptazymes, are collectively known as FNAs to emphasize their functions beyond the traditional genetic storage and transformations roles for DNA and RNA. Unlike DNA and RNA inside biological systems, FNAs are isolated via a combinatorial technique known as *in vitro* selection, or a process also known as systematic evolution of ligands by exponential enrichment (SELEX). The discovery of new functions of nucleic acids has not only resulted in major advances in the fields of molecular biology and biochemistry, but also revolutionized sensors designs for both *in vitro* and *in vivo* applications.[7–8]

Over the past decade, numerous FNAs-based nanomaterials have been developed.[9–12] Among these FNAs-based nanosystems, the functions of FNAs can be categorized into two types: diagnostic function and therapeutic function. For the diagnostic function, the FNAs serve either as the biorecognition ligands for direct sensing and imaging of the specific targets,[10] or as the biocatalysts to produce signal amplification for indirect sensing and imaging of other targets of interest.[13] On the other hand, for the therapeutic function, the FNAs could be directly used as the therapeutic drugs for some diseases,[14] or serve as the host of other therapeutic reagents,[15] including anti-cancer drugs, miRNAs, and siRNAs. As a result, the combination of the diagnostic and therapeutic functions of FNAs with the diverse and strong signal transduction of nanomaterials has become a major active area of

research with many exciting results. In this review, we will highlight recent advances in molecular engineering of functional nucleic acid-based nanomaterials, focusing on noble metal nanomaterials, carbon nanomaterials, and nucleic acids nanostructures, and other representative nanomaterials, as well as their applications toward *in vivo* studies (Figure 1).

2. Molecular Engineering of Nucleic Acid Enzyme-based Nanomaterials toward *In Vivo* Applications

Nucleic acid enzymes (NAEs) are a class of catalytic nucleic acids, which generally can be obtained by *in vitro* selection, and therefore are more stable and easier for modification and preparation than natural protein enzymes. Up to now, a large number of NAEs have been developed to catalyze a wide range of chemical reactions, in which RNA-cleaving NAEs have been the most extensively studied and widely used in biological applications,[16] due to their outstanding properties, such as generally catalytically efficient and easily integration with signal transduction nanomaterials via RNA cleavage. However, the most significant challenge for using NAEs *in vivo* is their nontoxic delivery while maintaining the functions. Over the past decade, by combining with a variety of nanomaterials, NAEs-based nanomaterials have been developed to achieve a large number of special applications toward *in vivo* studies.[16–17]

2.1 Integration of Nucleic Acid Enzymes with Noble Metal Nanomaterials

Noble metal nanomaterials, particularly gold nanoparticles (AuNPs), have attracted much attention during the past decades due of their excellent properties such as high stability, strong plasmonic effects, efficient catalysis and low cytotoxicity. Another significant advantages of using gold nanomaterials in *in vivo* applications is their use as carriers to facilitate the cellualr entry of other materials, such as DNA, anti-tumor drugs, or small organic dyes. Using this feature to their advantage, Yehl et al. synthesized multivalent 10–23 DNAzyme-AuNP conjugates (DzNPs) as shown in Figure 2A.[18] They have demonstrated that DzNPs are less susceptible to nuclease degradation, readily enter mammalian cells, and catalytically down-regulate GDF15 gene expression levels in breast cancer cells in an RNA interference-independent pathway. By using AuNPs as the carrier, some of the key limitations in the adoption of DNAzymes in *in vivo* application were addressed. Later in 2016, Somasuntharam et al. used a similar design to catalytically silence the gene expression of tumor necrosis factor-α (TNF-α) *in vivo* as a potential therapeutic for myocardial infarction (MI) (Figure 2B).[19] They demonstrated that DzNPs can serve as effective anti-inflammatory agents in the heart by regulating TNF-α expression in a rodent model of acute MI and confer therapeutic benefits to the damaged heart. This is the first example of DzNPs for viable delivery and gene regulation *in vivo*. Another smart strategy for DNAzyme based gene regulation was developed by He et al. using a dual-functional probe composed of AuNPs, catalytic Zn^{2+}-dependent DNAzyme, anticancer drug doxorubicin (Dox), targeted AS1411 aptamer and acid-decomposable ZnO QDs.[20] Using AS1411 aptamer for targeting the receptors involved in cellular entry, the probes could be selectively delivered into the HeLa cells through endocytosis, and then retained in the acidic endosomes or lysosomes, where the ZnO QDs were rapidly dissolved to release Zn^{2+}. The Zn^{2+} released activated the DNAzyme and led to substrate cleavage followed by drug release; at the same time, the

cleaved substrate were designed to complement with the overexpressed miR-21 in the HeLa cells, thereby downregulating the intracellular level.

In addition to gene regulation, NAEs-based AuNPs can also serve as probes for sensing and imaging metal ions inside cells. For instance, the first DNAzyme-based nanoprobe for imaging of metal ions in live cells was recently developed by Wu et al.[21] In their design, 13-nm AuNPs served not only as a carrier for uranyl-specific 39E DNAzyme and 39S DNAzyme substrate strand labeled with a Cy3 fluorophore at the 5′ end and a quencher at the 3′ end, but also as a quencher for the Cy3 fluorophore (Fig. 2C). Upon the addition of UO_2^{2+}, the DNAzyme cleaved the substrate strand to release the shorter Cy3-labeled substrate strand, and thereby increasing the fluorescence. Using the similar method, Li et al. designed a two-color fluorescence nanoprobe based on the DNAzymes modified AuNPs, and demonstrated the simultaneous on-site imaging of the Zn^{2+} and Cu^{2+} in living cells.[22] In addition to metal ions imaging in living cells, Yang el at. recently developed a DNAzyme-based two-photon imaging probe (TP-8–17ES−AuNP) for Zn^{2+} imaging in deep tissues with a penetration depth up to 160 μm,[23] by modifying a Zn^{2+}-specific DNAzyme (8–17) with a TP fluorophore and using AuNPs for intracellular delivery. Another significant advancement in intracellular imaging of metal ions was the “on-demand” activation of DNAzymes by light.[24–25] In this way, non-specific cleavage of DNAzymes during their delivery into cells can be prevented, and metal ion imaging can be controlled both temporally and spatially by light. One innovative example for light-controlled activation of DNAzyme-based nanoprobe was reported by Wang et al.,[26] where a near-infared (NIR) photothermal activation system was developed. The system composed of a three-stranded DNAzyme precusor (TSDP) covalently attached to gold nanoshells. In the ground state, the TSDP was inactive. Upon NIR illumination, the temperature increased and the hybridization keeping the DNAzyme inactivated denatured and the DNAzyme became activated. Finally, the activated DNAzyme catalyzed the metal-ion-dependent reaction, releasing the product containing a fluorophore.

Due to the sequence specificity of NAEs, another important application of NAEs-based gold nanomaterials is microRNA (miRNA) imaging and expression control. Regulation of miRNA expression has been shown to be involved in the initiation and progression of cancer, hence a potential target for cancer therapy. In light of this discovery, Zhang et al. developed a miRNA imaging and potential drug release approach using multicomponent nucleic acid enzymes (MNAzymes) conjugated on the surface of silica-coated gold nanorods (Figure 2D).[27] After cellular uptake, the targeted miR-21 and miR-145 hybridized to the binding arms of the MNAzyme, and activated the MNAzyme to cleave the fluorophore labeled substrate to generate a fluorescent signal for intracellular miRNA imaging. At the same time, the substrate cleavage triggered conformational change of the MNAzyme also served as an uncapping mechanism, leading to the release of the encapsulated chemotherapeutics. This work provided a general strategy for disease diagnosis, prognosis, and combo treatment using chemo- and gene therapy. Later, to further improve the sensitivity of miRNAs imaging inside cells, a number of amplified sensing platforms based on DNAzymes-AuNPs have been reported, including a AuNP-based DNAzyme motor,[28] a AuNP-based hairpin-locked-DNAzyme probe,[29] a AuNP-based DNAzyme nanomachine,[30] as well as a AuNP loaded split-DNAzyme probe.[31] These multitude of DNAzyme-

AuNP probes demonstrate a significant advancement toward *in vivo* amplified detection and imaging of various analytes.

2.2 Integration of Nucleic Acid Enzymes with Carbon Nanomaterials

Carbon nanomaterials, including carbon nanotubes (CNTs) and graphene, have gained substantial research interest in biomedical and bioanalytical fields because of their unique properties of good biocompatibility, high internalization efficiency, easy functionalization, excellent quenching ability to a broad range of fluorophores, and protection of conjugated DNA from enzymatic cleavage. In recent years, the integration of carbon nanomaterials with NAEs have been found to be practical in *in vivo* applications.

One promising direction is to use the carbon nanomaterials as a carrier to immobilize the NAEs. For example, Li et al. (Figure 3A) demonstrated a DNAzyme-based walker system as a controlled release platform for a therapeutic aptamer, AS1411, for breast cancer treatment.[32] In this system, the 10–23 DNAzyme (green) was first conjugated with a CdTe/CdS QD (orange), and then moved along the CNT track (black) in the presence of Mg^{2+}, leading to the release of the anticancer oligonucleotide AS1411 (light blue) from the anchor strand (navy). The released Cy5 dye labeled AS1411 (red) further formed a dimeric G-quadruplex structure in the presence of K^+, resulting in the anti-proliferation of MCF-7 cells.

In addition to serve as a carrier for NAEs, carbon nanomaterials can also be used to quench the fluorescence of fluorophores for imaging applications. For instance, Si et al. (Figure 3B) reported a NAEs-based nanoprobe, consisting of a DNAzyme, a hairpin probe, and graphene oxide (GO) as intracellular carrier and quencher, and demonstrated its application for the highly sensitive detection and simultaneous *in situ* imaging of Zn^{2+} and Cu^{2+} in living cells.[33] A signal amplification was obtained based on DNA self-assembly with DNAzyme catalysis in the presence of targeted metal ions. Later, Gao et al. developed another signal amplification strategy based on a proximity binding assay on GO integrated with Pb^{2+}-DNAzyme assistant probe recycling. Using this DNAzyme-GO nanoprobe, the detection and imaging of ATP in living cells was achieved.[34]

2.3 Integration of Nucleic Acid Enzymes with Nucleic Acids Nanostructures

Nucleic acid is also a viable material for the bottom-up assembly of nanoscale structures.[35] In recent decades, the emerging DNA nanotechnology provides a new route to fabricate various nucleic acids nanostructures via programmable DNA base pairing. Combining NAEs with nucleic acids nanostructures can provide new hybrid systems for *in vivo* applications. For instance, by modifying the edges of DNA tetrahedron with two DNAzymes, Zhou et al. (Figure 4A) designed a dual-color encoded DNAzyme-based nanoprobe for simultaniously detection of intracellular metal ions, UO_2^{2+} and Pb^{2+}.[36] However, a significant issue is that it needs an additional influx of metal ions to increase their intracellular concentration to detect a response. To address this issue, Wu et al. developed a novel method to amplify the signal from DNAzyme-catalyzed cleavage for detection of low levels of intracellular metal ions to better understand the roles of metal ions play in biolocial systems.[37] As shown in Figure 4B, by employing a hairpin structure, the probe consists of a Na^+-specific DNAzyme (NaA43) and a catalytic hairpin assemble (CHA). Upon activation from light and Na^+

exposure, the NaA43 DNAzyme cleaved the substrate and released a product stand, and this product strand triggered the subsequent CHA amplification to generate a turn-on fluorescence signal. This method can be employed to detect cellular metal ions in general with a DNAzyme and can have a potential to elucidate the roles of metal ions in biological systems.

Besides intracellular metal ion imaging, NAEs-based nucleic acids nanostructures have also been used for gene regulation,[38] enhanced cancer therapy,[39] and imaging of tumor-associated membrane protein.[40] For example, Jin et al. reported a NAEs based cancer therapeutic system with targeted genes silencing and cancer therapy by using a rolling circle amplification (RCA) method (Figure 4C).[39] In this construct, AS1411 aptamer, an EGR-1 (early growth response-1) DNAzyme and a surviving DNAzyme were self-assembled into a single DNA nanoflower (DNF) by using a long ssDNA product obtained from RCA and magnesium pyrophosphate. The resultant DNF was capable for cancer cell recognition, multiple gene silencing and induction of apoptosis. Similarly, by replacing magnesium pyrophosphate with a cationic polymer, the same group further developed a sponge-like platform for high efficiency photothermal therapy. (Figure 4D).[41] Similarly, Li et al. developed a multifunctional DNA nano-scorpion nanostructure using aptamers and DNAzyme for highly efficient targeted delivery and release of therapeutic mRNA for gene therapy.[42]

2.4 Integration of Nucleic Acid Enzymes with Other Nanomaterials

Magnetic nanoparticles (MNPs) have also been combined with NAEs for various *in vivo* applications. For example, Ryoo et al. reported an iron oxide nanoparticle-based system for the delivery of therapeutic DNAzyme for the treatment of hepatitis C (Figure 5A),[43] by down regulating NS3, a hepatitis C virus (HCV) gene, with no undesired immune responses or cytotoxicity. This delivery system was constructed by the conjugation of DNAzyme recognizing the NS3 sequence with iron oxide nanoparticles modified with cell penetrating peptide. They demonstrated that the DNAzyme conjugated nanoparticle system can be applied *in vivo* by showing the accumulation of these nanoparticles in hepatocytes. Recently, Bakshi et al. reported DNAzyme sensory system (MaBiDz) that can be activated upon a change in magnetic field and the system was demonstrated for intracellular sensing of specific mRNA (Figure 5B).[44] The magnetic field dependent DNAzyme activation was achieved by magnetic field triggered assembly of two components of the DNAzyme to form the active site for catalysis. The MaBiDz sensor was deployed successfully for rapid intracellular detection and imaging of a target mRNA biomarker for metastatic breast cancer. The application of MaBiDz sensor can further be expanded for mRNA regulation in a biomimetic organelle.

Recently, biodegradable MnO_2 nanosheets are also promoted as a new type of carrier to deliver NAEs for various diagnostic and therapeutic applications, with their appealing physicochemical properties such as acting as a good ssDNA carrier, an abundant reservoir of Mn^{2+} to activate 10–23 DNAzyme when reduced by intracellular glutathione (GSH), efficient quencher for broad-spectrum fluorescence, and finally, activatable magnetic resonance and fluorescence signaling for imaging applications. For example, Fan et al. have

developed a smart DNAzyme–MnO_2 nanosystem for gene silencing and intracellular imaging.[45] The system was constructed by conjugating photosensitizer Ce6 modified 10–23 DNAzyme with MnO_2 nanosheet to achieve a dual function gene silencing and photodynamic therapy (PDT) agent. This dual function agent demonstrated a remarkably improved therapeutic effect over that of gene silencing or PDT therapy alone. Additionally, Chen et al. (Figure 5C) further demonstrated that the combination of MnO_2-nanosheet with DNAzyme can also function as a catalytic DNA circuit generator for intracellular signal amplification to monitor DNA base-excision repairs in cells.[46] Similarly, employing MnO_2 nanosheets as DNAzyme carriers, the above group also introduced a general method for programming and assembly nanodevices with enzyme-activated DNAzymes (Figure 5D).[47] With this approach, it can not only monitor enzyme activity *in situ* but also enabled the implementation of cellular stages, behaviors, and pathways for basic science, diagnostic, and therapeutic applications as genetic circuits. Recently, silencing multiple genes in cells and *in vivo* was also reported by Li et al.[48] by using a novel DNAzymes-based nanocomposite (Figure 5E). In this system, cobalt oxyhydroxide (CoOOH) as a nanocarrier and oxidizing agent can be reduced by intracellular GSH, and the Co^{2+} as a reaction product and cofactor catalyzes 10–23 DNAzymes to cleave relevant mRNAs for gene silencing. The nanocomposite can simultaneously cleave three different tumor-related mRNAs in living cells and perform outstandingly towards the inhibition of cancer cells' migration, invasion and proliferation, and finally inhibit the tumor formation in a mouse model.

In addition to the above nanomaterials, NAEs have also been integrated with dendritic polyethylene–cationic poly(p-phenylene ethynylene),[49] metal−organic frameworks (MOFs),[50] UCNPs,[51] and cationic polypeptides,[52] for intracellular imaging of molecules, such as metal ions, miRNAs and messenger ribonucleic acids (mRNAs). As an example, Torabi et al.[52] reported the isolation of the first Na^+ specific RNA cleaving DNAzyme with highly selectivity, sensitivity, and efficiency (Figure 5F). The Na^+ DNAzyme was further converted into a catalytic beacon sensor for intracellular imaging Na^+ using an efficient cationic polypeptide delivery method. Furthermore, light-responsive activation was achieved by including a photocaging group at the cleavage site. Based on these studies, we summarize the representative reports focusing on NAEs integrated with other nanomaterials, as shown in Table 1.

3. Molecular Engineering of Aptamer-based Nanomaterials toward *In Vivo* Applications

Aptamers are single-stranded nucleic acid sequences that bind to specific targets through binding pockets formed with distinctive 3D structures. Similar to DNAzymes, aptamers are usually isolated through an *in vitro* SELEX or whole-cell based SELEX. Aptamers have several advantages including a wide variety of molecular targets with high binding specificity and affinity, rapid and reliable synthesis, good reproducibility, flexibility, and stable for long-term storage and transportation at ambient conditions. These advantages enable aptamers to be a promising molecular receptors, with diverse applications for *in vitro* detection and imaging of various targets.[53] Aside from *in vitro* detection, aptamers have also been explored for bioimaging *in vivo*, which is critical for disease diagnosis, prognosis,

patient stratification, and monitoring treatment response. Compared to antibodies, the convenient conjugation, rapid penetration and clearance represent the most significant advantages of aptamers for *in vivo* bioimaging.[53] In addition, aptamers can also be utilized as therapeutics due to its ability to bind and inhibit protein functions.[54] To date, a few therapeutic aptamers have made successful transition to clinical trials and commercial product, including pegaptanib for the treatment of age-related macular degeneration (AMD) and AS1411 for the treatment of cancer, and pegnivacogin as anticoagulants.

Despite these advances, however, few aptamer-based diagnostic or therapeutic products are on the market. From the perspective of *in vivo* applications, aptamers without specific modification are negatively charged and naturally repelled from the cell membrane which carries the same charge, hence, limiting their ability to cross the cell membrane.[55] Moreover, aptamers without protecting modifications are susceptible to degradation by nucleases inside the cellular matrix. As a result, it is necessary to combine and protect aptamers with additional carriers to improve cellular entry and resistance to nuclease. Nanomaterials are receiving significant attention in biochemical analysis and *in vivo* imaging due to their unique small sizes, large surface-to-volume, good biocompatibility, distinctive chemical, optical and electrical properties. Consequently, nanomaterials have been demonstrated to be outstanding delivery vehicles for their high loading efficiency of cargos, such as DNAs, drugs, or other molecules, as well as protection against nuclease degradation. Therefore, the integration of nanomaterials with aptamers have opened up exciting avenues for *in vivo* applications.[10]

3.1 Integration of Aptamers with Noble Metal Nanomaterials

Among various noble metal nanomaterials, gold nanomaterials are most intensely investigated as imaging contrast agents and nanocarriers.[56] As a result, the integration of aptamer with gold nanomaterials, such as Au nanorods (AuNRs),[57] Au nanoparticles (AuNPs),[58–72] Au nanocages,[73–74] Au nanostars (AuNSs),[75–76] hollow gold nanospheres (HAuNS),[77] and Au nanoclusters (Au NCs),[78] have been widely employed in *in vivo* applications in diverse areas, such as intracellular molecular imaging,[63, 68] cancer cell and tumor imaging,[57–58, 65–66, 69, 73, 77–78] targeted delivery of therapeutic cargos (e.g. anticancer drug,[74] protein,[61] gene[62]), and cancer therapy.[59–60, 70, 75–76] In one example, Huang et al. demonstrated the use of AuNRs as an efficient and robust multivalent platform for molecular assembly of aptamers for targeted cell imaging.[57] Based on the strong localized surface plasmon resonance of AuNPs, Javier et al. devised prostate-specific membrane antigen (PSMA)-aptamer modified gold nanoparticles for use as contrast agents for reflectance imaging of PSMA(+) and PSMA(−) cell lines.[58] Using the same PSMA aptamer, Kim et al. further designed the aptamer–AuNPs with loading of doxorubicin for additional chemotherapeutic effects against prostate cancer cells.[59] To improve the drug loading efficiency for cancer therapy, Zheng et al. engineered a spherical nucleic (SNA) acid by designing a cascade of hybridizations initiated from a AuNP-conjugated DNA initiator, and the cascade hybridization resulted in the formation of a nanoparticle shell composed of long DNA polymer.[60] By incorporating an aptamer to this SNA, the final construct showed high drug loading capacity as well as high selectivity. Later, Li et.al developed a system composed of fluorescent AuNPs conjugated with diatrizoic acid and AS1411 aptamer

(AS1411-DA-AuNPs),[65] which was successfully deployed as a molecular contrast agent to detect CL1–5 tumor by CT imaging. Recently, DNA-gadolinium-AuNPs that exhibit an improved T1 relaxivity and excellent cell uptake were developed by Nicholls et al (Figure 6A).[66] These nanoconjugates showed promising application for T1 MRI of transplanted human brain neural stem cells *in vivo*. Afterwards, Tang et al. constructed highly stabilized coresatellite Au nanoassemblies (CSAuNAs) by a hierarchical DNA-directed self-assembly strategy,[69] which can be selectively accumulated in the kidneys with satisfactory renal retention capability. Similarly, Si et al. developed versatile drug-loaded nanoprobes based on MUC1 aptamer integrated AuNPs, and further engineered telomerase-recognition sequence to the nanoprobes, enabling controllable drug release by intracellular telomerase.[71]

In addition to targeted cell imaging, aptamer-based gold nanomaterials have also been used for intracellular molecular imaging. For instance, by combining the structure-switching i-motif and the highly selective adenosine triphosphate (ATP) aptamer, Jin et al. developed a dual-stimuli responsive i-motif/nanoflares for ATP imaging in lysosomes.[63] Later, Chen et al.[68] (Figure 6B) reported the use of polyA-based SNA aptamer nanobeacons (PAaptNBs) that are functionalized with rationally designed polyadenine (polyA) diblock oligonucleotides, through which they achieved programmable engineering of PAaptNB for intracellular ATP imaging. In addition to ATP imaging, other molecules such as matrix metallopeptidase 3[64], potassium ions,[67] and Cytochrome c[72] have also been imaging using the aptamer-Au nanoprobes.

In addition to aptamer-gold nanomaterials for *in vivo* applications, silver nanomaterials have also been used,[79–85] among which nucleic acid-stabilized silver nanoclusters (Ag NCs) are the most attractive. Ag NCs possess good fluorescence properties, excellent photostability, subnanometer size, as well as low cytotoxicity. In addition, Ag NC fluorescence is highly dependent on the DNA sequence and are sensitive to oligonucleotide surroundings. These unique features make Ag NCs promising candidate for *in vivo* sensing and imaging. For example, Li et al. rationally connected AS1411 aptamer with poly(cytosine) via a -TTTTT- loop and employed it as the scaffold to synthesize Ag NCs through a one-step process.[80] The aptamer-Ag NCs nanoprobe not only exhibited good fluorescence properties for cell-type-specific imaging but also retained the anticancer nature of AS1411, and unexpectedly, demonstrated enhanced efficiency of growth inhibition to cancer cells compared with naked AS1411. By coupling Sgc8c aptamer-functionalized Ag NCs with biotinylated siRNA via a streptavidin bridge, Li et al. designed a multifunctional probe that enabled the specific delivery of siRNA into targeted cells for noninvasive imaging simultaneously.[81] Later, they also developed a second aptamer functionalized Ag NCs with “light-up” and “spectrum-shift” response for intracellular mRNA imaging.[82] Recently, to improve the resistance of Ag NCs to nuclease digestion, Han et al. (Figure 6C) utilized L-conformation of DNA (L-DNA) for the preparation of aptamer-Ag NCs.[83] Due to its absence in biological systems, L-DNA is resistant to nuclease digestion hence has resulted in NCs with much higher intracellular stability than those templated by regular DNA, thus making cell type specific imaging possible at physiological conditions, with much lower Ag NCs concentration than D-DNA-templated ones. Recently, Liu et al. synthesized target responsive Ag NCs beacon (ASNCB) for multiplex DNAs, small molecule, and protein sensing using a one-pot synthesis.[84] Incorporating an ATP aptamer to trigger ATP-responsive structure

transformation of ASNCB, ATP binding event induced ASNCB conformational transition and increased fluorescent signal of silver nanoclusters. Besides NCs, other silver nanomaterials, such as silver nanoparticles[86] and silver decahedral nanoparticles,[87] possess interesting properties, such as metal-enhanced fluorescence that increases the emission intensity of fluorophores nearby. Taking advantage of this feature, Li et al. (Figure 6D) developed a multifunctional theranostic agent based on the aptamer−silver conjugation, and applied it for cancer therapy and fluorescence-enhanced cell imaging.[86] Two aptamers, sgc8 aptamer targeting PTK7 receptor tyrosine kinase and TDO5 aptamer targeting heavy μ chains on the surface of Ramos cells, were used to functionalize the AgNPs, and showed a good performance toward the induction of apoptosis of targeted cells. In addition, using the fluorescent derivatives labeled aptamers for AgNP functionalization, the aptamer−silver conjugate can also be used for specific enhanced cell imaging via metal-enhanced fluorescence effect, while retaining their low cytotoxicity. A silver decahedral nanoparticles enhanced fluorescence resonance energy transfer (FRET) sensor for targeted cell imaging have also been developed by the same group.[87]

Hybrid metal nanomaterials have also been combined with aptamer for diverse *in vivo* applications. Shi et al.[88] (Figure 6E) designed an activatable theranostic nanoprobe (ATNP) via self-assembly of activatable aptamer probes (AAPs) on Au@Ag/Au NPs, and applied as a “nano-doctor” for image-guided cancer therapy both *in vitro* and *in vivo*. The Au@Ag/Au NPs served as the fluorescence quencher and optical heater, and exhibited a large absorption cross section from 400 to 1100 nm and ~ 4.5 times higher capacity for hyperthermia than Au NRs under 980 nm irradiation. By using an S6 aptamer against A549 cancer as the model, the AAP sequence was designed and optimized, which not only showed excellent target recognition ability, but also successfully achieved selective fluorescence activation. In addition, by introducing a target-triggered signal alteration mechanism into the diagnosis principle, this “nano-doctor” substantially enhanced the imaging contrast and shortened the detection time, leading to a fast and potent photothermal therapy (PTT) of cancer. In another case, aptamer coated Cu–Au alloy nanostructures for *in vivo* cancer theranostics have been reported by Ye et al. (Figure 6F).[89] The integration of Cu and Au not only solved the problem of functionalization of Cu nanomaterial, but also greatly improved the photostability of the Au nanomaterials, while the introduction of aptamers enabled the efficient localization and accumulation of the nanoprobes in cancer cells and tissues, resulting in the simultaneous fluorescent molecular imaging and NIR PTT of the target cancer. More recently, Hu et al.[90] reported another fluorescent monometallic Ag nanohybrids (Ag NHs) synthesized via polycytosine mediated Ag NCs biomineralization on Ag NPs. The aptamer-functionalized Ag NHs served as an efficient therapeutic agent and can induce reactive oxygen species generation leading apoptosis once it’s delivered into target cells.

Other hybrid metal nanomaterials-aptamer system, such as AuNP/Ag NCs,[91] DNA-origami–AuNRs hybrid,[92] Mn(II) silver-aptamer clusters,[93] and Au NCs/chitosan NPs,[94] have also been reported for imaging and therapeutic applications. For instance, inspired by the intriguing properties of DNA origami and AuNRs, Du et al.[92] (Figure 6G) designed an optoacoustic imaging (OAI) agent via self-assembly of AuNRs onto DNA-origami nanostructures. The resulting AuNRs–DNA-nanostructure hybrid combined the advantages

of AuNRs with those of the DNA-origami structure, and served as a unique probe and an efficient contrast agent in OAI, and thereby improved the imaging quality with decreased dose. Simultaneously, the NIR-responsive AuNRs–DNA-nanostructure hybrid was applied for PTT, and effectively inhibited tumor regrowth and prolonged the survival of diseased mice.

3.2 Integration of Aptamers with Carbon Nanomaterials

Graphene oxide (GO), especially nanosized GO (nGO) with a size < 100 nm and a narrow distribution, features several unique properties: first, nGO is a super quencher for a wide range of fluorophores via FRET or non-radiative dipole−dipole coupling. Second, the affinity of DNA adsorption on nGO is mediated via π−π stacking and hydrogen bonding, which is strong enough to attain a low background yet weak enough to allow rapid probe release in the presence of target molecules. Third, nGO is readily internalized by living cells with efficient cell membrane permeability. Finally, nGO has low cytotoxicity. Therefore, nGO has emerged as an outstanding platform in the past few years to interface with aptamers for *in vivo* applications.[95–96]

In one example, Tan et al.[97] performed ATP live-cell imaging with greatly improved signal-to-background ratio by using an ATP aptamer molecular beacon functionalized nGO (Figure 7A). To achieve more accurate quantification, a control ssDNA was designed to be released from the GO as it encountered cellular proteins; and the signal from the ssDNA served as an internal reference for calibration and ratiometric quantification. Although the internal standard improved quantification, the non-specific release of reference ssDNA probe from GO cannot be avoided, introducing certain degree of inaccuracy. To resolve this issue, Liu et al.[98] covalently attached a fluorophore modified ATP aptamer to nGO via an extra amine modification on the aptamer. The resultant nGO ATP probe was used for intracellular ATP detection. Another example was provided by Wang et al.[99] who developed a multiple aptamer/nGO based sensing platform for simultaneous monitoring of ATP and GTP *in situ*. Recently, Yi et al.[100] (Figure 7B) went a step further and used the deeper penetration depth of two-photon microscopy to develop an aptamer-two photon dye (TP dye)/GO two-photon excitation fluorescent sensing conjugate for ATP imaging in zebrafish. This approach had advantages of the exceptional quenching capability of GO for the proximate TP dyes and the higher affinity of single-stranded aptamer on GO than the aptamer−target complex, showing great potential for *in vivo* applications in medical research and clinical diagnostics.

In addition to the ATP imaging, aptamer responsive fluorescent nanocomposites containing QDs and GO were further developed by Zhang et al.,[101] and applied to monitor the cellular entry and the drug delivery processes *in situ*. With the extremely high two-photon absorption cross-section from GO, Pramanik et al.[102] reported a selective two-photon imaging of SK-BR-3 breast tumor cell in second biological transparency windows using 1100 nm wavelength. Chen et al.[103] (Figure 7C) developed a fluorescent aptamer nanosensor to image the activation of cytochrome c (Cyt c). The reported strategy relied on the construction and spatially specific cytosolic delivery of a nanosensor assembled from fluorophore conjugated DNA aptamers on PEGylated GO. The release of Cyt c in cytosol would bind and dissociated the aptamer from GO, resulting in an increased fluorescence

signal. The nanosensor enabled real-time visualization of the Cyt c release kinetics and direct identification of the regulators for apoptosis.

Apart from nGO, other types of carbon nanomaterials, including porous GO membranes,[96] CNTs,[104–105] carbon nanodots,[106] graphene QDs,[107], and mesoporous carbon nanospheres,[108] have also been integrated with aptamers for selective cell isolation, imaging, and drug delivery. As an example, using fluorophore-labeled aptamer and single-walled carbon nanotube, Yan et al.[105] developed an activatable aptamer probe for cancer cell (Figure 7D). Through π-stacking and proximity-induced energy transfer, without any target, the probe will be quenched in its free state. Upon binding to cell surface receptors, probe was released and fluorescence signal was activated. *In vivo* studies further confirmed that specifically activated fluorescence was observed in CCRF-CEM tumors. Compared to "always on" probes, this probe had greatly reduced background signals, thus resulting in much higher contrast in the image. Later, Li et al.[108] reported a mesoporous carbon nanosphere that can deliver drugs to tumors and image tumor biomarkers in real time.

3.3 Integration of Aptamers with Nucleic Acids Nanostructures

Molecular engineering of aptamers with nucleic acids nanostructures have been developed in the past decade in a wide range of biomedical studies. For instance, Shi et al.[109] (Figure 8A) reported an activatable aptamer beacon probe (AAP) for targeting membrane proteins of living cancer cells and for imaging cancer tissues in mice. The AAP consisted of three fragments: a cancer-targeted aptamer sequence (A-strand), a poly T linker (T-strand), and a short DNA sequence (C-strand) complementary to a part of the A-strand with a fluorophore and quencher attached to both termini. When the beacon was applied in a CCRF-CEM mouse xenograft model, the tumor-specific antigen PTK1 on the surface of the tumor cells was selectively imaged 60 min after administration, facilitating sensitive detection of early-stage cancer. Later, Zhang et al.[110] designed a controllable aptamer-based self-assembled DNA dendrimer for high affinity targeting, bioimaging and drug delivery. Another smart split aptamer-based activatable theranostic probe was reported as "nanodoctor" for cancer-activated *in vivo* imaging and *in situ* drug release (Figure 8B).[111] This nanodoctor exhibited tunable *in vivo* stability, in which rapid diagnosis with contrast-enhanced image was achieved in 5 min.

Recently, DNA nanoflowers (NFs) were synthesized by co-precipitation of magnesium pyrophosphate and a rolling circle replication (RCR) DNA product. Due to densely packed DNA building blocks, these NFs are resistant to nuclease degradation, denaturation, and dissociation at extremely low concentrations, hence highly suitable for intracellular imaging and targeted delivery. For instance, Hu et al.[112] reported an aptamer FRET NFs synthesized using RCR for simultaneous imaging of multiple targets using single excitation, in additional to targeted anti-tumor drug delivery. Also, Wu et al.[113] engineered a switchable aptamer micelle flare by self-assembly of an aptamer-diacyl-lipid chimera, to monitor intracellular ATP. Similarly, Zhang et al.[114] developed a molecular beacon (MB) based micelle (a-MBM-DOX) for MDR1 through the self-assembly of diacyl-lipid–MB (L–MB) and doxorubicin (DOX) molecules. These a-MBMs were demonstrated to enter cells efficiently and only release the drug after they have bypass the MDR barrier. Hence, this

system can have great promise for an all-in-one micelle probe to carry out sequential mRNA imaging and image-guided therapy.

Another emerging 3D self-assembled DNA nanostructure is DNA tetrahedron, which has been used for intracellular imaging, cellular imaging and targeted delivery.[115] DNA tetrahedron possesses many interesting properties, including good structural rigidity, excellent biocompatibility, nuclease resistance, and rapid cell entry, contributing to its application for cellular applications. Taking these features, Pei et al.[116] developed an ATP aptamer tetrahedron, for ATP imaging in live cells (Figure 8C). Using the similar method, Xie et al.[117] reported self-assembled DNA tetrahedron molecular beacon for intracellular tumor-related mRNA and ATP detection. Combining the excellent biological properties of DNA nanostructures with low background split aptamers, Zheng et al.[118] developed a FRET-based functional DNA triangular-prism for ATP sensing in living cells. Similarly, RNA tetrahedron has been recently reported by Li et al. (Figure 8D),[119] in which EGFR aptamers were placed at the edges of the RNA tetrahedrons with high precision without disrupting the overall structure. These aptamer-RNA tetrahedrons demonstrated tumor-specific enrichment in orthotopic MDA-MB-231 tumor-bearing mice after systemic administration. Using the similar strategies, they have also developed a series of aptamer-guided *in vivo* targeting platform for the treatment of prostate cancer,[120] glioblastoma,[121] gastric cancer,[122] colorectal cancer,[123] and head/neck cancer.[124] Together, several aptamer integrated RNA nanostructures have demonstrated the superior capability for selective targeting of diseased tissues over other nanotechnology platforms.

In addition to intracellular analysis, another exciting application of aptamer functionalized nucleic acids nanostructures is toward targeted delivery of therapeutics. For instance, Abnous et al.[125] reported a novel aptamer-based DNA diamond nanostructure for *in vivo* targeted delivery of epirubicin to cancer cells. Jin et al.[126] used the DNA aptamer-modified oligoguanine quadruplex nanostructures for targeted delivery. The aptamer-tethered oligoguanine nucleotides self-assembled to form Y-shaped DNA structures, which were shown to have strong potential for cells specific drug delivery and improved therapeutic effects. Porciani et al.[127] engineered a cell-internalizing aptamer nanostructure that enables targeted delivery of large functional RNAs in cancer cell lines. This platform exploited cell-internalizing aptamers to accomplish cell type specific delivery, along with the fluorescence properties of RNA mimics of GFP as surrogates for other large RNA-based payloads. To further improve the affinity and stability of aptamer-based probes for *in vivo* applications, Lei et al.[128] designed a novel theranostic strategy of DNA nanotriangle-scaffolded multivalent split activatable aptamer probe (NTri-SAAP), which combines advantages of programmable self-assembly, multivalent effect and target-activatable architecture. The NTri-SAAP increased doxorubicin loading capacity by ~5 times, which further realized a high anti-tumor efficacy *in vivo* with 81.95% inhibition but no obvious body weight loss. Another critical challenge for the therapeutic use of aptamer-based DNA nanomaterials is the precise delivery to tumor sites in a highly controlled manner to minimize its side effects. To overcome the challenge, Li et al.[129] constructed a DNA nanorobotic system using DNA origami (Figure 8E). The tubular nanorobot was formed with a foldable origami sheet has thrombin molecules linked to it via DNA aptamers and fasteners capable of binding to nucleolin. In tumour vasculature, the nucleolin interaction could undo the fasteners and

thereby release the thrombin to trigger fibrin clot formation, leading to thrombosis and clot formation causing blood vessel occlusion. Bi et al.[130] reported the synthesis of DNA nanohydrogels using a target-catalyzed DNA four-way junction as building units. These DNA nanohydrogels are readily functionalized by incorporating with aptamers, bioimaging agents, and drug loading sites, which thus are served as efficient platform for simultaneously imaging of miRNA and targeted drug delivery for cancer therapy. Other *in vivo* applications including the monitoring of RNA−RNA hybridization,[131] *in vivo* aptamer photoregulation,[132] specific imaging of cell-surface glycosylation,[133] and mRNA detection,[134] have also been developed based on the integration of aptamers with DNA nanostructures, such as *Split-Broccoli* assembles,[131] a photolabile oligonucleotide complex,[132] hybridization chain reaction (HCR) nanoassemblies,[133] and DNA nanotube.[134]

In addition to the fluorescent imaging, aptamers have been also integrated with other imaging modalities for enhanced *in vivo* imaging. For instance, photoacoustic (PA) imaging has emerged as a new imaging modality capable of achieving submillimeter resolution at depths up to 7–10 cm. The first DNA aptamer-based PA probe has been recently developed by Zhang et al.,[135] in which a thrombin binding aptamer was hybridized with IRDye 800CW-labeled and IRDye QC-1 quencher-labeled ssDNA to form a DNA duplex structure with efficient contact quenching (Figure 8F). Assembly and disassembly of the DNA complex by the target of interest can inhibit the contact quenching, resulting in a change of the PA signal at its two maximum absorption wavelengths. The aptamer-based PA probe exhibited an enhanced and specific ratiometric change in PA signals toward thrombin injection *in vivo*, demonstrating the first aptamer-based activatable PA probe for advanced molecular imaging in living mice.

3.4 Integration of Aptamers with Other Nanomaterials

QDs feature several unique optical properties, including broad absorption spectra, narrow photoluminescence bandwidths, high quantum yield, low photobleaching, and resistance to chemical degradation. The functionalization of QDs with aptamers can be realized via covalently conjugation,[136–140] electrostatic interactions,[141] biotin-streptavidin interactions,[142–143] and aptamer-templated QDs synthesis.[144–145] These aptamer-QDs have been increasingly utilized as biological imaging and labeling probes for targeted cell detection and imaging,[136,138–139] drug delivery,[136] gene silencing,[141] and imaging-guided tumor therapy.[137, 140] For instance, Zhang et al.[144] offered a strategy to synthesize aptamer-functionalized Zn^{2+} doped CdTe QDs through a facile one-pot hydrothermal route, and have successfully applied it in active tumor-targeted imaging *in vitro* and *in vivo*. Wei et al.[145] went a step further and reported a new type of aptamer templated heterobivalent QD nanoprobes with the ability to target and image two spatially isolated cancer markers present on the cell surface (e.g. nucleolin) and in the cell cytosol (e.g. mRNA). Bypassing endolysosomal sequestration, this type of QD nanoprobes undergo macropinocytosis following the nucleolin targeting and then translocate to the cytosol for mRNA targeting. Recently, aptamer functionalized NIR Ag2S nanodot has been synthesized through HCR signal amplification,[146] and further combined with immune-magnetic spheres for the efficient isolation and detection of circulating tumor cells (CTCs) in whole blood. To improve the imaging sensitivity of aptamer-QDs, Li et al.[147] further employed HCR for

bottom-up construction of aptamer-QDs polymers, which enabled both multidentate targeting and multi-QD-based signal amplification. Another water-soluble Ag2S NIR fluorescent QDs have been synthesized for specific cancer imaging and PTT using a designed aptamer (Apt43) as template.[148] The synthesized Apt43-Ag2S QDs exhibited strong fluorescence emission and absorption in the NIR region and high photothermal conversion capabilities, and have been applied for the *in vivo* ablation of tumors. In addition, by incorporating two different aptamers into a hybrid micellar QDs, intracellular ATP-activatable aptamer-QDs has been reported by Shen et al.,[149] which enabled dual fluorescence imaging and targeted photodynamic therapy of tumor (Figure 9A).

Aptamer functionalized UCNPs have also been developed toward targeted bioimaging and delivery,[150–153] intracellular imaging,[154] *in vivo* sensing,[155] and photodynamic therapy.[156] However, most of the UCNPs are capped with hydrophobic ligands, such as oleylamine, and thereby it remains challenging to prepare biocompatible UCNPs with specific molecular recognition capabilities. To address this issue, Li et al.[157] developed a facile one-step ligand exchange strategy to prepare uniform aptamer-modified UCNPs as versatile bioprobes. The DNA-UCNPs were capable of crossing cell membranes without the need of transfection agents, and their use as agents for targeted imaging of cancer cells has been realized. Later, the same group have also developed a hetero-assembled DNA-AuNP/UCNP system,[158] which maintains both plasmonic resonance of AuNPs and fluorescent properties of UCNPs, allowing targeted dual-modality imaging of cancer cells using an aptamer. Very recently, Zhao et al.[155] reported a rationally designed, synthetic DNA nanodevice that can detect ATP in living cells and animals in an upconversion luminescence-activatable manner (Figure 9B). The nanodevice consists of a UV light-activatable aptamer probe, and lanthanide-doped UCNPs which act as the nanotransducers to operate the device in response to NIR light. They have demonstrated that the nanodevice not only enables efficient cellular delivery of the aptamer probe into live cells, but also allows the temporal control over its fluorescent sensing activity for ATP by NIR light irradiation *in vitro* and *in vivo*. Aptamer-UCNPs based targeted bioimaging and photodynamic therapy have been recently developed by Yuan et al.[159] by using an aptamer-guided G-Quadruplex DNA carrier and NIR light. Another example came from Fang et al.[160] who utilized the aptamer-conjugated UCNPs for effective isolation and sensitive detection of CTCs assisted by magnetic separation. Another exciting application of aptamer-UCNPs has been reported by Wu et al.,[161] in which profiling cell surface protein-specific glycoforms was realized based on a single excitation-dual LRET (D-LRET) system that consists of UCNPs as a donor and Alexa Fluor 555/660 as two different fluorescence acceptors (Figure 9C).

In the past decade, various aptamer functionalized magnetic nanomaterials have been developed,[162–163] and applied for diverse *in vivo* applications, including isolation and detection of cancer cells,[164–166] sensing and imaging,[167–172] delivery of therapeutic agents,[173] and cancer imaging and therapy.[174–181] As an example, Westmeyer et al.[167] designed an aptamer-based MRI system that can detect the activity of cell secreted alkaline phosphatase. This method was based on the enzymatic dephosphorylation of AMP to adenosine, which in turn can disrupt a DNA duplex that aggregates MNPs, thereby separating the MNPs and reduce their collective superparamagnetism. In addition, Zhang et al.[168] have developed a core-triple shell structured multi-functional nanoprobe $Fe_3O_4/SiO_2/$

CdSeTe@ZnS−SiO_2/polydopamine with strong fluorescence and a fast magnetic response for specifically recognizing, fluorescently labeling, and magnetically sorting target tumor cells on a microfluidic chip. Li et al.[174] proposed an aptamer functionalized Fe_3O_4@Au nanorose with five distinct functions, integrating aptamer-based targeting, MRI, optical imaging, photothermal therapy and chemotherapy into one single probe. Yang et al.[173] (Figure 9D) constructed a smart magnetic nanoaptamer based on the assembly of DNA-templated Fe_3O_4, hydrophobic dye, HIF-1α and glucose transporter 1 aptamers, and siRNA. The resulting magnetic nanoaptamer can transport siRNA to breast cancer cells or tissues for the attenuation of HIF-1α and ATP, and thereby inhibits the growth of cancer cells *in vivo*.

In addition to the above mentioned aptamer-nanomaterials systems, other types of aptamer-based nanomaterials, such as liposome,[182–186] silica nanomaterials,[187–194] polymer nanomaterials,[195–198] MOFs,[199] dendrimers,[200–201] micellar nanoparticles,[202–203] gadolinium oxide nanoparticles,[204–205] calcium carbonate nanostructure,[206] polydopamine nanospheres,[207–208] MoS_2 nanoplates,[209] lipid-based nanobubbles,[210] dipeptide nanoparticles,[211] aggregation-induced emission organic dots,[212] and MnO_2 nanosheet,[213] have been engineered as promising candidates toward *in vivo* applications in diverse areas. Based on these studies, we summarize the representative reports focusing on aptamers integrated with other nanomaterials, as shown in Table 2.

4. Molecular Engineering of Aptazyme-based Nanomaterials toward *In Vivo* Applications

Aptazymes are ligand-activate self-cleaving ribozymes that contain both an aptamer domain and a ribozyme domain, which can readily convert the binding signals to more distinct signals of enzyme activities (Figure 10A),[214] such as self-cleavage or ligase.[215] In the absence of the target ligand, the enzymatic activity of the catalytic element cannot be expressed due to inappropriate structural folding. However, the introduction of the target ligand can induce the adaptive folding of the aptamer domain, leading to the structural formation of the catalytic domain and subsequently its activation. Breaker and coworkers were the pioneers in coupling catalytic domains to aptameric recognition domains,[216] in which the binding of the target ligand to the aptamer induces the catalytic event (ligation or cleavage). Based on this strategy, aptazymes are able to directly transduce molecular recognition into a quantitative catalytic event. Taking advantages of highly specific recognition property of aptamers and signal amplification property of NAEs via multiple-turnover reactions, aptazymes have demonstrated their great promise in many *in vitro* applications.[217–219]

However, in contrast to the broad *in vivo* applications of NAEs and aptamers, there are considerably less studies on aptazymes for similar applications.[211] This difference was mainly due to two reasons from both fundamental and technical aspect. First, most aptazyme sensors are developed by artificial design using known NAEs and aptamers rather than by more efficient combinatorial selection strategies, and this fundamental limitation thereby results in extensive trial-and-error and optimization procedures when identifying an aptazyme sensor with target-dependent response. Second, many of these design strategies for

aptazymes often involve changes in the active sites or binding arms of FNAs to introduce aptamer sequences into NAEs. Such strategies have been successfully applied for target detection, but the insertion of aptamers may interfere the activity of the NAEs and make it difficult to apply the same design approach rationally to other NAEs and aptamer pairs, because of the dramatically different properties of each NAEs and aptamer. So far, unfortunately, few aptazymes have been integrated with nanomaterials toward *in vivo* applications.

4.1 Integration of Aptazymes with Noble Metal Nanomaterials

The integration of noble metal nanomaterials with aptazymes for amplified molecular probing in living cells was first reported by Yang et al. (Figure 10B),[220] where they combined gold nanoparticles with a well-characterized ATP-specific aptazyme strand, composed of Mg^{2+}-dependent 10–23 DNAzyme and ATP aptamer. The target molecule can activate the aptazyme and then cleave and release the fluorophore-labeled substrate strands from the AuNP, resulting in fluorescence enhancement. They demonstrated that the aptazyme-AuNP can readily enter living cells and realize intracellular ATP detection at physiological concentration of Mg^{2+}, with no additional Mg^{2+} required.

4.2 Integration of Aptazymes with Nucleic Acids Nanostructures

Aptazymes-embedded DNA nanostructures have been developed for various *in vivo* applications.[221–222] For instance, Ogawa et al. reported aptazyme-based riboswitches based on a theophylline aptamer and an anti-ribosome binding site (RBS) sequence.[223] They integrated the aptazyme with a RBS and a complementary anti-RBS, resulted in an artificial ribozyme-based riboswitch. In this way, the ligand-dependent hammerhead ribozyme (HHR) mediated cleavage reaction could remove the anti-RBS domain from the transcript, releasing the RBS and thus enabling translation of the mRNA both *in vitro* and *in vivo*. Later, Wieland et al. presented an improved hammerhead aptazyme design that enables ribozymes to act as artificial riboswitches in bacteria.[224] In other cases, it was demonstrated that aptazymes can also be used to control the activity of tRNAs,[225] regulation of miRNAs,[226] and 16S Ribosomal RNA in bacteria.[222] Later, aptazymes have been demonstrated for diverse applications, including construction of synthetic gene networks in yeast,[227] and regulation of transgene expression,[228] or virus replication in mammalian cell culture.[229] Recently, rational design of aptazyme riboswitches for efficient control of gene expression in mammalian cells was developed by Zhong et al. (Figure 10C).[230] These aptazymes efficiently regulated adeno-associated virus (AAV)-vectored transgene expression in cultured mammalian cells and mice, highlighting one application of these broadly usable regulatory switches.

Additionally, combining with CRISPR technologies, aptazyme-based nanomaterials have showed the ability to improve the dynamically control of gene expression. For example, Tang et al. embedded self-cleaving catalytic RNA aptazymes in the sgRNA (Figure 10D), [231] which block the sgRNA spacer sequence until exposure to a ligand. These aptazyme-embedded guide RNAs exhibited three unique features: small molecule-controlled nuclease-mediated genome editing, small molecule-controlled base editing, and small molecule-dependent transcriptional activation in mammalian cells.

5. Summary and Perspectives

In summary, we have provided a review of exciting advancements of molecular engineering of nanomaterials with FNAs, including NAEs, aptamers, and aptazymes. These FNAs-nanomaterials have shown several unique features that make them as promising candidates toward diverse *in vivo* applications. For example, different therapeutic agents, such as chemotherapeutic drugs, photosensitizers and siRNA, have been integrated with aptamers for targeted cancer therapy based on different therapeutic strategies.[232] In addition, FNAs-based theranostic agents with both imaging and therapeutic functions, have also been developed to increase diagnosis accuracy and therapy efficiency. Finally, the combination of different nanomaterials into hybrid nanomaterials yielded new nanocomposites with multi-functionalities for various *in vivo* applications. Another emerging technique for this field, is that researchers are now capable of encoding and self-assembling nanostructures inside live cells.[233] This opens up the possibility of encoding new FNAs-nanomaterials inside cells and even whole organisms, providing a new direction for the development of efficient targeted diagnostics and therapeutics *in vivo*.

Despite such remarkable progress in engineering FNAs-nanomaterials toward *in vivo* applications, there remains several challenges limiting their clinical applications. First, most of the reported NAEs and aptamers are selected and applied in *in vitro* studies. The *in vivo* behaviors of these FNAs may be far more complicated than our present knowledge, and it is of high probability that FNAs selected *in vitro* lose their functionalities to some extent towards their targets in living systems. Therefore, an innovation of SELEX protocols for FNAs with more desired performance under *in vivo* applications is urgently needed.

Second, for intracellular or *in vivo* imaging, rationally designed FNAs-nanomaterials can greatly increase the sensitivity and specificity for biomolecular recognition because of the well-controlled probe density, orientation, and surface passivation.[234] In this way, these FNAsnanomaterials could provide a versatile and efficient platform for imaging of various targets *in vivo*. In addition, the development of NIR emitting FNAs-nanomaterials is another trick for *in vivo* biosensing and imaging, since the tissues, blood, and water exhibit minimal absorption and autofluorescence in the NIR region. However, it remains a challenge to develop a NIR emitting nanomaterials with high fluorescent quantum yield, and therefore innovative approaches are needed to facilitate the improve of fluorescent quantum yields in the NIR range. Meanwhile, the biocompatibility of the FNAs-nanomaterials is also important to improve the precision and accuracy for the detection of biological targets in complex sample matrices toward *in vivo* applications. The integration of FNAs with nanomaterials may introduce the biosafety risk, such as toxicity and inflammation induced by nanomaterials, which requires further intensive studies before the translation of FNAs-based nanomaterials into clinical applications.

Finally, for therapeutic purpose, the cellular uptake, endosomal escape, and *in vivo* stability of FNAs-nanomaterials still need to be optimized. We anticipate that new designs based on these foundations will be developed to further improve sensing, imaging, and drug delivery. Another challenge is to improve the delivery of FNAs-nanomaterials in a precisely controlled manner to meet the needs of a given *in vivo* application, and additionally direct

the FNAs-nanomaterials to the subcellular molecular imaging as well as more efficient diagnostics and therapeutics *in vivo*. At the same time, applications of FNAs-based nanomaterials in clinical trials should be speeded up so as to pave the way for virtual target therapy into reality. Overcoming these challenges would further broaden the scope of *in vivo* applications of FNAs-nanomaterials and potentially facilitate the translation of them to the clinic.

Acknowledgements

The Lu group research described in this review has been supported by US National Institute of Health (GM124316 and MH110975). GlucoSentient R&D related to this review has been supported by NIH (MH111337–01).

Biographies

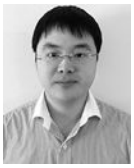

JingJing Zhang received his PhD degree in chemistry under the supervision of Prof. Jun-Jie Zhu from the School of Chemistry and Chemical Engineering, Nanjing University in 2010. Currently, he works as a postdoctoral research associate in the group of Prof. Yi Lu at the University of Illinois Urbana-Champaign since March 2012. His research interests focus on interfacing carbon and gold nanomaterials with biological systems, and developing novel tools for imaging, sensing and diagnostics.

Tian Lan Received his Ph.D degree in biochemistry under the supervision of Prof. Yi Lu from the school of molecular and cellular biology at the University of Illinois at Urbana-Champaign in 2011. Currently, he is working as the lead scientist at GlucoSentient on diagnostic product development.

Yi Lu received his BS degree from Peking University in 1986, and a PhD degree from the University of California at Los Angeles in 1992 under Professor Joan S. Valentine. After 2 years of postdoctoral research in Professor Harry B. Gray’s group at the California Institute of Technology, Lu started his own independent career in the Department of Chemistry at the University of Illinois at Urbana-Champaign in 1994. He is now a Jay and Ann Schenck

Professor of Chemistry in the Departments of Chemistry, Biochemistry, Bioengineering and Materials Science and Engineering. He is also a member of the Center for Biophysics and Computational Biology and Beckman Institute for Advanced Science and Technology. His research interests include a) design and engineering of functional metalloproteins as environmentally benign catalysis in renewable energy generation and pharmaceuticals; b) fundamental understanding of DNAzymes and their applications in environmental monitoring, medical diagnostics, and targeted drug delivery; and c) employing principles from biology for directed assembly of nanomaterials with controlled morphologies and their applications in imaging and medicine.

References

[1]. Zhang JJ, Cheng FF, Li JJ, Zhu JJ, Lu Y, Nano Today 2016, 11, 309. [PubMed: 27818705]

[2]. Samanta A, Medintz IL, Nanoscale 2016, 8, 9037. [PubMed: 27080924]

[3]. Sivaram AJ, Wardiana A, Howard CB, Mahler SM, Thurecht KJ, Adv. Healthcare Mater 2018, 7, 1700607.

[4]. Angell C, Kai MX, Xie SB, Dong XY, Chen Y, Adv. Healthcare Mater 2018, 7, 1701189.

[5]. Kim J, Jang D, Park H, Jung S, Kim DH, Kim WJ, Adv. Mater 2018, 30, 1707351.

[6]. Liu JW, Cao ZH, Lu Y, Chem. Rev 2009, 109, 1948. [PubMed: 19301873]

[7]. Li J, Li F, Pei H, Wang LH, Huang Q, Fan CH, Adv. Mater. Ser 2015, DOI: Book_Doi 10.1002/978111899892293.

[8]. Pei H, Zuo XL, Zhu D, Huang Q, Fan CH, Acc. Chem. Res 2014, 47, 550. [PubMed: 24380626]

[9]. Ihms HE, Lu Y, Methods. Mol. Biol 2012, 848, 297. [PubMed: 22315076]

[10]. Meng HM, Liu H, Kuai HL, Peng RZ, Mo LT, Zhang XB, Chem. Soc. Rev 2016, 45, 2583. [PubMed: 26954935]

[11]. Wang ZD, Lu Y, J. Mater. Chem 2009, 19, 1788.

[12]. Liang H, Zhang XB, Lv YF, Gong L, Wang RW, Zhu XY, Yang RH, Tan WH, Acc. Chem. Res 2014, 47, 1891. [PubMed: 24780000]

[13]. Zhang JJ, Catalysts 2018, 8, 550.

[14]. Zhou JH, Rossi J, Nat. Rev. Drug Discov 2017, 16, 181. [PubMed: 27807347]

[15]. Hu QQ, Wang S, Wang LH, Gu HZ, Fan CH, Adv. Healthcare Mater 2018, 7, 1701153.

[16]. Torabi SF, Lu Y, Curr. Opin. Biotechnol 2014, 28, 88. [PubMed: 24468446]

[17]. Zhao XH, Meng HM, Gong L, Qiu LP, Zhang XB, Tan WH, Chinese J Anal. Chem 2015, 43, 1611.

[18]. Yehl K, Joshi JP, Greene BL, Dyer RB, Nahta R, Salaita K, ACS Nano 2012, 6, 9150. [PubMed: 22966955]

[19]. Somasuntharam I, Yehl K, Carroll SL, Maxwell JT, Martinez MD, Che PL, Brown ME, Salaita K, Davis ME, Biomaterials 2016, 83, 12. [PubMed: 26773660]

[20]. He ZM, Zhang PH, Li X, Zhang JR, Zhu JJ, Sci. Rep 2016, 6, 22737. [PubMed: 26956167]

[21]. Wu P, Hwang K, Lan T, Lu Y, J. Am. Chem. Soc 2013, 135, 5254. [PubMed: 23531046]

[22]. Li L, Feng J, Fan Y, Tang B, Anal. Chem 2015, 87, 4829. [PubMed: 25853631]

[23]. Yang C, Yin X, Huan SY, Chen L, Hu XX, Xiong MY, Chen K, Zhang XB, Anal. Chem 2018, 90, 3118. [PubMed: 29409318]

[24]. Hwang K, Wu PW, Kim T, Lei L, Tian SL, Wang YX, Lu Y, Angew. Chem. Int. Ed. Engl 2014, 53, 13798. [PubMed: 25314680]

[25]. Wang X, Feng M, Xiao L, Tong A, Xiang Y, ACS Chem Biol 2016, 11, 444. [PubMed: 26669486]

[26]. Wang W, Satyavolu NSR, Wu Z, Zhang JR, Zhu JJ, Lu Y, Angew. Chem 2017, 56, 6798. [PubMed: 28471018]

[27]. Zhang P, He Z, Wang C, Chen J, Zhao J, Zhu X, Li CZ, Min Q, Zhu JJ, ACS Nano 2015, 9, 789. [PubMed: 25525669]

[28]. Peng H, Li XF, Zhang H, Le XC, Nat. Commun 2017, 8, 14378. [PubMed: 28262725]

[29]. Yang Y, Huang J, Yang X, He X, Quan K, Xie N, Ou M, Wang K, Anal. Chem 2017, 89, 5850. [PubMed: 28503919]

[30]. Liu J, Cui M, Zhou H, Yang W, ACS Sens. 2017, 2, 1847. [PubMed: 29181969]

[31]. Wu Y, Huang J, Yang X, Yang Y, Quan K, Xie N, Li J, Ma C, Wang K, Anal. Chem 2017, 89, 8377. [PubMed: 28718626]

[32]. Li F, Cha TG, Pan J, Ozcelikkale A, Han B, Choi JH, Chembiochem. 2016, 17, 1138. [PubMed: 27059426]

[33]. Si H, Sheng R, Li Q, Feng J, Li L, Tang B, Anal. Chem 2018, 90, 8785. [PubMed: 29973043]

[34]. Gao FL, Wu J, Yao Y, Zhang Y, Liao XJ, Geng DQ, Tang DQ, RSC Adv. 2018, 8, 28161.

[35]. Li ZH, Wang J, Li YX, Liu XW, Yuan Q, Mat. Chem. Front 2018, 2, 423.

[36]. Zhou W, Liang W, Li D, Yuan R, Xiang Y, Biosens. Bioelectron 2016, 85, 573. [PubMed: 27236722]

[37]. Wu Z, Fan H, Satyavolu NSR, Wang W, Lake R, Jiang JH, Lu Y, Angew. Chem 2017, 56, 8721. [PubMed: 28557357]

[38]. Belter A, Rolle K, Piwecka M, Fedoruk-Wyszomirska A, Naskret-Barciszewska MZ, Barciszewski J, Sci. Rep 2016, 6, 24516. [PubMed: 27079911]

[39]. Jin Y, Li ZH, Liu HF, Chen SZ, Wang F, Wang L, Li N, Ge K, Yang XJ, Liang XJ, Zhang JC, Npg Asia Mater. 2017, 9, 365.

[40]. Chen X, Zhao J, Chen T, Gao T, Zhu X, Li G, Theranostics 2018, 8, 1075. [PubMed: 29464000]

[41]. Jin Y, Liang LN, Sun XJ, Yu GS, Chen SZ, Shi ST, Liu HF, Li ZH, Ge K, Liu DD, Yang XJ, Zhang JC, Npg Asia Mater. 2018, 10, 373.

[42]. Li D, Mo F, Wu J, Huang Y, Zhou H, Ding S, Chen W, Sci. Rep 2018, 8, 10196. [PubMed: 29976947]

[43]. Ryoo SR, Jang H, Kim KS, Lee B, Kim KB, Kim YK, Yeo WS, Lee Y, Kim DE, Min DH, Biomaterials 2012, 33, 2754. [PubMed: 22206595]

[44]. Bakshi SF, Guz N, Zakharchenko A, Deng H, Tumanov AV, Woodworth CD, Minko S, Kolpashchikov DM, Katz E, Nanoscale 2018, 10, 1356. [PubMed: 29297526]

[45]. Fan H, Zhao Z, Yan G, Zhang X, Yang C, Meng H, Chen Z, Liu H, Tan W, Angew. Chem 2015, 54, 4801. [PubMed: 25728966]

[46]. Chen F, Bai M, Cao K, Zhao Y, Wei J, Zhao YX, Adv. Funct. Mater 2017, 27, 1702748.

[47]. Chen F, Bai M, Cao K, Zhao Y, Cao XW, Wei J, Wu N, Li J, Wang LH, Fan CH, Zhao YX, ACS Nano 2017, 11, 11908. [PubMed: 29045785]

[48]. Li N, Li Y, Gao X, Yu Z, Pan W, Tang B, Chem. Comm 2017, 53, 4962. [PubMed: 28422198]

[49]. Zhang L, Huang HY, Xu N, Yin QH, J. Mater. Chem. B 2014, 2, 4935.

[50]. Yi JT, Chen TT, Huo J, Chu X, Anal. Chem 2017, 89, 12351. [PubMed: 29083869]

[51]. Yang ZL, Loh KY, Chu YT, Feng RP, Satyavolu NSR, Xiong MY, Huynh SMN, Hwang K, Li LL, Xing H, Zhang XB, Chelma YR, Gruebele M, Lu Y, J. Am. Chem. Soc 2018, 140, 17656.

[52]. Torabi SF, Wu P, McGhee CE, Chen L, Hwang K, Zheng N, Cheng J, Lu Y, Proc. Natl. Acad. Sci. USA 2015, 112, 5903. [PubMed: 25918425]

[53]. Xing H, Wong NY, Xiang Y, Lu Y, Curr. Opin. Chem. Biol 2012, 16, 429. [PubMed: 22541663]

[54]. Lao YH, Phua KKL, Leong KW, ACS Nano 2015, 9, 2235. [PubMed: 25731717]

[55]. Dong JT, Zhao MP, Trac-Trends in Anal. Chem 2016, 80, 190.

[56]. Wang CC, Wu SM, Li HW, Chang HT, Chembiochem. 2016, 17, 1052. [PubMed: 26864481]

[57]. Huang YF, Chang HT, Tan WH, Anal. Chem 2008, 80, 567. [PubMed: 18166023]

[58]. Javier DJ, Nitin N, Levy M, Ellington A, Richards-Kortum R, Bioconjug. Chem 2008, 19, 1309. [PubMed: 18512972]

[59]. Kim D, Jeong YY, Jon S, ACS Nano 2010, 4, 3689. [PubMed: 20550178]

[60]. Zheng J, Zhu G, Li Y, Li C, You M, Chen T, Song E, Yang R, Tan W, ACS Nano 2013, 7, 6545. [PubMed: 23841478]

[61]. Ryou SM, Yeom JH, Kang HJ, Won M, Kim JS, Lee B, Seong MJ, Ha NC, Bae J, Lee K, J Control Release 2014, 196, 287. [PubMed: 25450403]

[62]. Chen Z, Zhang L, He Y, Li Y, ACS Appl. Mater. Interfaces 2014, 6, 14196. [PubMed: 25019323]

[63]. Jin F, Zheng J, Liu C, Yang S, Li Y, Li J, Lian Y, Yang R, Analyst 2014, 139, 3714. [PubMed: 24905584]

[64]. Lee SE, Chen Q, Bhat R, Petkiewicz S, Smith JM, Ferry VE, Correia AL, Alivisatos AP, Bissell MJ, Nano Lett. 2015, 15, 4564. [PubMed: 26039492]

[65]. Li CH, Kuo TR, Su HJ, Lai WY, Yang PC, Chen JS, Wang DY, Wu YC, Chen CC, Sci. Rep 2015, 5, 15675. [PubMed: 26507179]

[66]. Nicholls FJ, Rotz MW, Ghuman H, MacRenaris KW, Meade TJ, Modo M, Biomaterials 2016, 77, 291. [PubMed: 26615367]

[67]. Yang Y, Huang J, Yang X, Quan K, Xie N, Ou M, Tang J, Wang K, Chem. Comm 2016, 52, 11386. [PubMed: 27709181]

[68]. Chen L, Chao J, Qu X, Zhang H, Zhu D, Su S, Aldalbahi A, Wang L, Pei H, ACS Appl. Mater. Interfaces 2017, 9, 8014. [PubMed: 28221021]

[69]. Tang L, Yu G, Tan L, Li M, Deng X, Liu J, Li A, Lai X, Hu J, Sci. Rep 2017, 7, 8553. [PubMed: 28819188]

[70]. Zhang D, Zheng A, Li J, Wu M, Wu L, Wei Z, Liao N, Zhang X, Cai Z, Yang H, Liu G, Liu X, Liu J, Theranostics 2017, 7, 164. [PubMed: 28042325]

[71]. Si H, Wang L, Li Q, Li X, Li L, Tang B, Chem. Comm 2018, 54, 8277. [PubMed: 29989641]

[72]. Tang J, Huang C, Shu J, Zheng J, Ma D, Li J, Yang R, Anal. Chem 2018, 90, 5865. [PubMed: 29595257]

[73]. Demeritte T, Fan Z, Sinha SS, Duan J, Pachter R, Ray PC, Chem. Eur. J 2014, 20, 1017. [PubMed: 24339156]

[74]. Wang W, Chen C, Li X, Wang S, Luo X, Chem. Comm 2015, 51, 9109. [PubMed: 25939588]

[75]. Jo H, Youn H, Lee S, Ban C, J. Mater. Chem. B 2014, 2, 4862.

[76]. Li Y, Wang XL, Gao L, Hu P, Jian LC, Ren TY, Fu R, Yang DW, Jiang XH, J. Mater. Sci 2018, 53, 14138.

[77]. Melancon MP, Zhou M, Zhang R, Xiong C, Allen P, Wen X, Huang Q, Wallace M, Myers JN, Stafford RJ, Liang D, Ellington AD, Li C, ACS Nano 2014, 8, 4530. [PubMed: 24754567]

[78]. Chen D, Li B, Cai S, Wang P, Peng S, Sheng Y, He Y, Gu Y, Chen H, Biomaterials 2016, 100, 1. [PubMed: 27236844]

[79]. Chen LQ, Xiao SJ, Peng L, Wu T, Ling J, Li YF, Huang CZ, J. Phys. Chem. B 2010, 114, 3655. [PubMed: 20112983]

[80]. Li JL, Zhong XQ, Cheng FF, Zhang JR, Jiang LP, Zhu JJ, Anal. Chem 2012, 84, 4140. [PubMed: 22482827]

[81]. Li JJ, Wang WJ, Sun DF, Chen JN, Zhang PH, Zhang JR, Min QH, Zhu JJ, Chem. Sci 2013, 4, 3514.

[82]. Li JJ, You J, Zhuang YP, Han CP, Hu JF, Wang A, Xu K, Zhu JJ, Chem. Commun 2014, 50, 7107.

[83]. Han GM, Jia ZZ, Zhu YJ, Jiao JJ, Kong DM, Feng XZ, Anal. Chem 2016, 88, 10800. [PubMed: 27797508]

[84]. Liu GL, Lo JJ, Feng DQ, Zhu JJ, Wang W, Anal. Chem 2017, 89, 1002. [PubMed: 28105835]

[85]. Yin JJ, He XX, Wang KM, Xu FZ, Shangguan JF, He DG, Shi H, Anal. Chem 2013, 85, 12011. [PubMed: 24266455]

[86]. Li H, Hu HT, Zhao YJ, Chen X, Li W, Qiang WB, Xu DK, Anal. Chem 2015, 87, 3736. [PubMed: 25686206]

[87]. Li H, Hu HT, Xu DK, Anal. Chem 2015, 87, 3826. [PubMed: 25764443]

[88]. Shi H, Ye XS, He XX, Wang KM, Cui WS, He DG, Li D, Jia XK, Nanoscale 2014, 6, 8754. [PubMed: 24953128]

[89]. Ye XS, Shi H, He XX, Yu YR, He DG, Tang JL, Lei YL, Wang KM, Nanoscale 2016, 8, 2260. [PubMed: 26743815]

[90]. Hu SQ, Ye BY, Tang HL, Wu F, Yi XY, Yi TT, Wu DH, Wu L, Wang JX, J. Mater. Chem. B 2018, 6, 1187.

[91]. Zhu YJ, Li WJ, Hong ZY, Tang AN, Kong DM, J. Mater. Chem. B 2017, 5, 9229.

[92]. Du Y, Jiang Q, Beziere N, Song LL, Zhang Q, Peng D, Chi CW, Yang X, Guo HB, Diot G, Ntziachristos V, Ding BQ, Tian J, Adv. Mater 2016, 28, 10000. [PubMed: 27679425]

[93]. Mu WY, Xiao XX, Chen TT, Chen QY, J. Mater. Chem. B 2016, 4, 5284.

[94]. Guo XL, Zhuang QF, Ji TJ, Zhang YL, Li CJ, Wang YQ, Li H, Jia HY, Liu Y, Du LB, Carbohyd. Polym 2018, 195, 311.

[95]. Huang RC, Chiu WJ, Lai IPJ, Huang CC, Sci. Rep 2015, 5, 10292. [PubMed: 25973571]

[96]. Nellore BPV, Kanchanapally R, Pramanik A, Sinha SS, Chavva SR, Hamme A, Ray PC, Bioconjug. Chem 2015, 26, 235. [PubMed: 25565372]

[97]. Tan XH, Chen T, Xiong XL, Mao Y, Zhu GZ, Yasun E, Li CM, Zhu Z, Tan WH, Anal. Chem 2012, 84, 8622. [PubMed: 22978721]

[98]. Liu ZB, Chen SS, Liu BW, Wu JP, Zhou YB, He LY, Ding JS, Liu JW, Anal. Chem 2014, 86, 12229. [PubMed: 25393607]

[99]. Wang Y, Tang LH, Li ZH, Lin YH, Li JH, Nat. Protoc 2014, 9, 1944. [PubMed: 25058642]

[100]. Yi M, Yang S, Peng ZY, Liu CH, Li JS, Zhong WW, Yang RH, Tan WH, Anal. Chem 2014, 86, 3548. [PubMed: 24592855]

[101]. Zhang L, Xiao SJ, Zheng LL, Li YF, Huang CZ, J. Mater. Chem. B 2014, 2, 8558.

[102]. Pramanik A, Chavva SR, Fan Z, Sinha SS, Priya B, Nellore V, Ray PC, J. Phys. Chem. Lett 2014, 5, 2150. [PubMed: 26270507]

[103]. Chen TT, Tian X, Liu CL, Ge J, Chu X, Li YF, J. Am. Chem. Soc 2015, 137, 982. [PubMed: 25548948]

[104]. Khan SA, Kanchanapally R, Fan Z, Beqa L, Singh AK, Senapati D, Ray PC, Chem. Commun 2012, 48, 6711.

[105]. Yan LA, Shi H, He XX, Wang KM, Tang JL, Chen MA, Ye XS, Xu FZ, Lei YL, Anal. Chem 2014, 86, 9271. [PubMed: 25153687]

[106]. Lee CH, Rajendran R, Jeong MS, Ko HY, Joo JY, Cho S, Chang YW, Kim S, Chem. Commun 2013, 49, 6543.

[107]. Wang XJ, Sun X, He H, Yang H, Lao J, Song YZ, Xia YQ, Xu H, Zhang XD, Huang F, J. Mater. Chem. B 2015, 3, 3583.

[108]. Li CY, Qian M, Wang SS, Jiang HL, Du YL, Wang JX, Lu WY, Murthy N, Huang RQ, Theranostics 2017, 7, 3319. [PubMed: 28900512]

[109]. Shi H, He XX, Wang KM, Wu X, Ye XS, Guo QP, Tan WH, Qing ZH, Yang XH, Zhou B, Proc. Natl. Acad. Sci. USA 2011, 108, 3900. [PubMed: 21368158]

[110]. Zhang HM, Ma YL, Xie Y, An Y, Huang YS, Zhu Z, Yang CYJ, Sci. Rep 2015, 5.

[111]. Lei YL, Tang JL, Shi H, Ye XS, He XX, Xu FZ, Yan LA, Qiao ZZ, Wang KM, Anal. Chem 2016, 88, 11699. [PubMed: 27807977]

[112]. Hu R, Zhang XB, Zhao ZL, Zhu GZ, Chen T, Fu T, Tan WH, Angew. Chem 2014, 53, 5821. [PubMed: 24753303]

[113]. Wu CC, Chen T, Han D, You MX, Peng L, Cansiz S, Zhu GZ, Li CM, Xiong XL, Jimenez E, Yang CJ, Tan WH, ACS Nano 2013, 7, 5724. [PubMed: 23746078]

[114]. Zhang RL, Gao S, Wang ZL, Han D, Liu L, Ma QJ, Tan WH, Tian J, Chen XY, Adv. Funct. Mater 2017, 27, 1701027. [PubMed: 29056886]

[115]. Xie NL, Liu SY, Yang XH, He XX, Huang J, Wang KM, Analyst 2017, 142, 3322. [PubMed: 28835943]

[116]. Pei H, Liang L, Yao GB, Li J, Huang Q, Fan CH, Angew. Chem 2012, 51, 9020. [PubMed: 22887892]

[117]. Xie NL, Huang J, Yang XH, Yang YJ, Quan K, Ou M, Fang HM, Wang KM, ACS Sens. 2016, 1, 1445.

[118]. Zheng XF, Peng RZ, Jiang X, Wang YY, Xu S, Ke GL, Fu T, Liu QL, Huan SY, Zhang XB, Anal. Chem 2017, 89, 10941. [PubMed: 28931278]

[119]. Li H, Zhang KM, Pi FM, Guo SJ, Shlyakhtenko L, Chiu W, Shu D, Guo PX, Adv. Mater 2016, 28, 7501. [PubMed: 27322097]

[120]. Binzel DW, Shu Y, Li H, Sun MY, Zhang QS, Shu D, Guo B, Guo PX, Mol. Ther 2016, 24, 1267. [PubMed: 27125502]

[121]. Lee TJ, Haque F, Shu D, Yoo JY, Li H, Yokel RA, Horbinski C, Kim TH, Kim SH, Kwon CH, Nakano I, Kaur B, Guo PX, Croce CM, Oncotarget 2015, 6, 14766. [PubMed: 25885522]

[122]. Cui DX, Zhang CL, Liu B, Shu Y, Du T, Shu D, Wang K, Dai FP, Liu YL, Li C, Pan F, Yang YM, Ni J, Li H, Brand-Saberi B, Guo PX, Sci. Rep 2015, 5.

[123]. Rychahou P, Haque F, Shu Y, Zaytseva Y, Weiss HL, Lee EY, Mustain W, Valentino J, Guo PX, Evers BM, ACS Nano 2015, 9, 1108. [PubMed: 25652125]

[124]. Shu Y, Haque F, Shu D, Li W, Zhu ZQ, Kotb M, Lyubchenko Y, Guo PX, RNA 2013, 19, 767. [PubMed: 23604636]

[125]. Abnous K, Danesh NM, Ramezani M, Lavaee P, Jalalian SH, Yazdian-Robati R, Emrani AS, Hassanabad KY, Taghdisi SM, RSC Adv. 2017, 7, 15181.

[126]. Jin H, Kim MG, Ko SB, Kim DH, Lee BJ, Macgregor RB, Shim G, Oh YK, Nanoscale 2018, 10, 7511. [PubMed: 29637946]

[127]. Porciani D, Cardwell LN, Tawiah KD, Alam KK, Lange MJ, Daniels MA, Burke DH, Nat. Commun 2018, 9.

[128]. Lei YL, Qiao ZZ, Tang JL, He XX, Shi H, Ye XS, Yan L, He DG, Wang KM, Theranostics 2018, 8, 4062. [PubMed: 30128036]

[129]. Li SP, Jiang Q, Liu SL, Zhang YL, Tian YH, Song C, Wang J, Zou YG, Anderson GJ, Han JY, Chang Y, Liu Y, Zhang C, Chen L, Zhou GB, Nie GJ, Yan H, Ding BQ, Zhao YL, Nat. Biotechnol 2018, 36, 258. [PubMed: 29431737]

[130]. Bai S, Xiu B, Ye JY, Dong Y, ACS Appl. Mater. Interfaces 2015, 7, 23310. [PubMed: 26420675]

[131]. Alam KK, Tawiah KD, Lichte MF, Porciani D, Burke DH, ACS Synth. Biol 2017, 6, 1710. [PubMed: 28548488]

[132]. Li LL, Tong R, Chu HH, Wang WP, Langer R, Kohane DS, Proc. Natl. Acad. Sci. USA 2014, 111, 17099. [PubMed: 25404344]

[133]. Yuan BY, Chen YY, Sun YQ, Guo QP, Huang J, Liu JB, Meng XX, Yang XH, Wen XH, Li ZH, Li L, Wang KM, Anal. Chem 2018, 90, 6131. [PubMed: 29696967]

[134]. Ji XT, Lv HY, Guo JY, Ding CF, Luo XL, Chem. Eur. J 2018, 24, 10171.

[135]. Zhang JJ, Smaga LP, Satyavolu NSR, Chan J, Lu Y, J. Am. Chem. Soc 2017, 139, 17225. [PubMed: 29028325]

[136]. Bagalkot V, Zhang L, Levy-Nissenbaum E, Jon S, Kantoff PW, Langer R, Farokhzad OC, Nano Lett. 2007, 7, 3065. [PubMed: 17854227]

[137]. Savla R, Taratula O, Garbuzenko O, Minko T, Control J. Release 2011, 153, 16.

[138]. Hu DH, Zhang PF, Gong P, Lian SH, Lu YY, Gao DY, Cai LT, Nanoscale 2011, 3, 4724. [PubMed: 21989776]

[139]. Jie GF, Zhao YB, Qin YQ, Chem. Asian J 2014, 9, 1261. [PubMed: 24616365]

[140]. Du W, Yuan Y, Wang L, Cui YS, Wang H, Xu HQ, Liang GL, Bioconjug. Chem 2015, 26, 2571. [PubMed: 26580576]

[141]. Bagalkot V, Gao XH, ACS Nano 2011, 5, 8131. [PubMed: 21936502]

[142]. Chu TC, Shieh F, Lavery LA, Levy M, Richards-Kortum R, Korgel BA, Ellington AD, Biosens. Bioelectron 2006, 21, 1859. [PubMed: 16495043]

[143]. Chen LQ, Xiao SJ, Hu PP, Peng L, Ma J, Luo LF, Li YF, Huang CZ, Anal. Chem 2012, 84, 3099. [PubMed: 22423600]

[144]. Zhang CL, Ji XH, Zhang Y, Zhou GH, Ke XL, Wang HZ, Tinnefeld P, He ZK, Anal. Chem 2013, 85, 5843. [PubMed: 23682757]

[145]. Wei W, He XW, Ma N, Angew. Chem 2014, 53, 5573. [PubMed: 24740625]

[146]. Ding CP, Zhang CL, Yin XY, Cao XY, Cai MF, Xian YZ, Anal. Chem 2018, 90, 6702. [PubMed: 29722265]

[147]. Li Z, He XW, Luo XC, Wang L, Ma N, Anal. Chem 2016, 88, 9355. [PubMed: 27649276]

[148]. Gao JW, Wu CL, Deng D, Wu P, Cai CX, Adv. Healthcare Mater 2016, 5, 2437.

[149]. Shen YZ, Tian Q, Sun YD, Xu JJ, Ye DJ, Chen HY, Anal. Chem 2017, 89, 13610. [PubMed: 29181974]

[150]. Zhou L, Li ZH, Ju EG, Liu Z, Ren JS, Qu XG, Small 2013, 9, 4262. [PubMed: 23843269]

[151]. Zhou L, Chen ZW, Dong K, Yin ML, Ren JS, Qu XG, Biomaterials 2014, 35, 8694. [PubMed: 25002259]

[152]. Deng KR, Hou ZY, Li XJ, Li CX, Zhang YX, Deng XR, Cheng ZY, Lin J, Sci. Rep 2015, 5, 7851. [PubMed: 25597762]

[153]. Wu Y, Li D, Zhou F, Liang H, Liu Y, Hou W, Yuan Q, Zhang X, Tan W, Chem. Sci 2018, 9, 5427. [PubMed: 30009014]

[154]. Ma L, Liu F, Lei Z, Wang Z, Biosens. Bioelectron 2017, 87, 638. [PubMed: 27619527]

[155]. Zhao J, Gao JH, Xue WT, Di ZH, Xing H, Lu Y, Li LL, J. Am. Chem. Soc 2018, 140, 578. [PubMed: 29281270]

[156]. Han S, Samanta A, Xie X, Huang L, Peng J, Park SJ, Teh DBL, Choi Y, Chang YT, All AH, Yang Y, Xing B, Liu X, Adv. Mater 2017, 29, 1700244.

[157]. Li LL, Wu PW, Hwang K, Lu Y, J. Am. Chem. Soc 2013, 135, 2411. [PubMed: 23356394]

[158]. Li LL, Lu Y, J. Am. Chem. Soc 2015, 137, 5272. [PubMed: 25853565]

[159]. Yuan Q, Wu Y, Wang J, Lu DQ, Zhao ZL, Liu T, Zhang XB, Tan WH, Angew. Chem 2013, 52, 13965. [PubMed: 24281972]

[160]. Fang S, Wang C, Xiang J, Cheng L, Song XJ, Xu LG, Peng R, Liu Z, Nano Res. 2014, 7, 1327.

[161]. Wu N, Bao L, Ding L, Ju HX, Angew. Chem 2016, 55, 5220. [PubMed: 27001418]

[162]. Rosen JE, Chan L, Shieh DB, Gu FX, Nanomed. Nanotechnol 2012, 8, 275.

[163]. Zhang L, Dong WF, Sun HB, Nanoscale 2013, 5, 7664. [PubMed: 23877222]

[164]. Herr JK, Smith JE, Medley CD, Shangguan D, Tan W, Anal. Chem 2006, 78, 2918. [PubMed: 16642976]

[165]. Smith JE, Medley CD, Tang ZW, Shangguan D, Lofton C, Tan WH, Anal. Chem 2007, 79, 3075. [PubMed: 17348633]

[166]. Li JJ, Wang S, Wu C, Dai Y, Hou PF, Han CP, Xu K, Biosens. Bioelectron 2016, 86, 1047. [PubMed: 27501342]

[167]. Westmeyer GG, Durocher Y, Jasanoff A, Angew. Chem 2010, 49, 3909. [PubMed: 20414908]

[168]. Zhang PH, Cao JT, Min QH, Zhu JJ, ACS Appl. Mater. Interfaces 2013, 5, 7417. [PubMed: 23823645]

[169]. Yang B, Chen BB, He M, Yin X, Xu C, Hu B, Anal. Chem 2018, 90, 2355. [PubMed: 29308635]

[170]. Ko HY, Choi KJ, Lee CH, Kim S, Biomaterials 2011, 32, 1130. [PubMed: 21071077]

[171]. Wang CX, Zhou JJ, Wang P, He WS, Duan HW, Bioconjug. Chem 2016, 27, 815. [PubMed: 26859517]

[172]. Zhu HT, Zhang LR, Liu YF, Zhou YP, Wang K, Xie XD, Song L, Wang DQ, Han CL, Chen QY, Sci. Rep 2016, 6, 39245. [PubMed: 27976736]

[173]. Yang R, Mu WY, Chen QY, Wang Q, Gao J, ACS Biomater. Sci. Eng 2018, 4, 2606.

[174]. Li CM, Chen T, Ocsoy I, Zhu GZ, Yasun E, You MX, Wu CC, Zheng J, Song EQ, Huang CZ, Tan WH, Adv. Funct. Mater 2014, 24, 1772. [PubMed: 25530745]

[175]. Wang AZ, Bagalkot V, Vasilliou CC, Gu F, Alexis F, Zhang L, Shaikh M, Yuet K, Cima MJ, Langer R, Kantoff PW, Bander NH, Jon SY, Farokhzad OC, Chemmedchem 2008, 3, 1311. [PubMed: 18613203]

[176]. Chen T, Shukoor MI, Wang RW, Zhao ZL, Yuan Q, Bamrungsap S, Xiong XL, Tan WH, ACS Nano 2011, 5, 7866. [PubMed: 21888350]

[177]. Yu MK, Kim D, Lee IH, So JS, Jeong YY, Jon S, Small 2011, 7, 2241. [PubMed: 21648076]

[178]. Wu P, Gao Y, Zhang H, Cai CX, Anal. Chem 2012, 84, 7692. [PubMed: 22925013]

[179]. Fan Z, Senapati D, Singh AK, Ray PC, Mol. Pharmaceut 2013, 10, 857.

[180]. Fan Z, Shelton M, Singh AK, Senapati D, Khan SA, Ray PC, ACS Nano 2012, 6, 1065. [PubMed: 22276857]

[181]. Roy K, Kanwar RK, Kanwar JR, Biomaterials 2015, 71, 84. [PubMed: 26318819]

[182]. Cao ZH, Tong R, Mishra A, Xu WC, Wong GCL, Cheng JJ, Lu Y, Angew. Chem 2009, 48, 6494. [PubMed: 19623590]

[183]. Xing H, Tang L, Yang XJ, Hwang K, Wang WD, Yin Q, Wong NY, Dobrucki LW, Yasui N, Katzenellenbogen JA, Helferich WG, Cheng JJ, Lu Y, J. Mater. Chem. B 2013, 1, 5288. [PubMed: 24159374]

[184]. Zhang KC, Liu M, Tong XY, Sun N, Zhou L, Cao Y, Wang JE, Zhang HL, Pei RJ, Biomacromolecules 2015, 16, 2618. [PubMed: 26212580]

[185]. Xing H, Zhang CL, Ruan G, Zhang JJ, Hwang K, Liu Y, Anal. Chem 2016, 88, 1506. [PubMed: 26750765]

[186]. Kim MW, Jeong HY, Kang SJ, Choi MJ, You YM, Im CS, Lee TS, Song IH, Lee CG, Rhee KJ, Lee YK, Park YS, Sci. Rep 2017, 7, 9474. [PubMed: 28842588]

[187]. Li LL, Yin Q, Cheng JJ, Lu Y, Adv. Healthcare Mater 2012, 1, 567.

[188]. Tang L, Yang XJ, Dobrucki LW, Chaudhury I, Yin Q, Yao C, Lezmi S, Helferich WG, Fan TM, Cheng JJ, Angew. Chem 2012, 51, 12721. [PubMed: 23136130]

[189]. Li HN, Mu YW, Lu JS, Wei W, Wan YK, Liu SQ, Anal. Chem 2014, 86, 3602. [PubMed: 24576151]

[190]. Wang XY, Song PS, Peng L, Tong AJ, Xiang Y, ACS Appl. Mater. Interfaces 2016, 8, 609. [PubMed: 26653325]

[191]. Cai L, Chen ZZ, Chen MY, Tang HW, Pang DW, Biomaterials 2013, 34, 371. [PubMed: 23084552]

[192]. Zhang YA, Guo S, Cheng SB, Ji XH, He ZK, Biosens. Bioelectron 2017, 94, 478. [PubMed: 28342376]

[193]. Li LL, Xie MY, Wang J, Li XY, Wang C, Yuan Q, Pang DW, Lu Y, Tan WH, Chem. Commun 2013, 49, 5823.

[194]. Tan JT, Yang N, Zhong LP, Tan J, Hu ZX, Zhao Q, Gong WL, Zhang ZH, Zheng R, Lai ZQ, Li YM, Zhou CF, Zhang GQ, Zheng D, Zhang Y, Wu SY, Jiang XL, Zhong JH, Huang Y, Zhou SF, Zhao YX, Theranostics 2017, 7, 4862. [PubMed: 29187909]

[195]. Farokhzad OC, Khademhosseini A, Yon SY, Hermann A, Cheng JJ, Chin C, Kiselyuk A, Teply B, Eng G, Langer R, Anal. Chem 2005, 77, 5453. [PubMed: 16131052]

[196]. Gao HL, Qian J, Cao SJ, Yang Z, Pang ZQ, Pan SQ, Fan L, Xi ZJ, Jiang XG, Zhang QZ, Biomaterials 2012, 33, 5115. [PubMed: 22484043]

[197]. Gao HL, Qian J, Yang Z, Pang ZQ, Xi ZJ, Cao SJ, Wang YC, Pan SQ, Zhang S, Wang W, Jiang XG, Zhang QZ, Biomaterials 2012, 33, 6264. [PubMed: 22683171]

[198]. Jung YK, Woo MA, Soh HT, Park HG, Chem. Commun 2014, 50, 12329.

[199]. Wang HS, Li J, Li JY, Wang K, Ding Y, Xia XH, Npg Asia Mater. 2017, 9, 354.

[200]. Mohammadzadeh P, Cohan RA, Ghoreishi SM, Bitarafan-Rajabi A, Ardestani MS, Sci. Rep 2017, 7, 11832. [PubMed: 28928437]

[201]. Yan HH, Gao XH, Zhang YF, Chang WJ, Li JH, Li XW, Du Q, Li C, ACS Appl. Mater. Interfaces 2018, 10, 17047. [PubMed: 29708329]

[202]. Tian JW, Ding L, Ju HX, Yang YC, Li XL, Shen Z, Zhu Z, Yu JS, Yang CJ, Angew. Chem 2014, 53, 9544. [PubMed: 25045069]

[203]. Wang DL, Liu B, Ma Y, Wu CW, Mou QB, Deng HP, Wang RB, Yan DY, Zhang C, Zhu XY, J. Am. Chem. Soc 2017, 139, 14021. [PubMed: 28945366]

[204]. Li JJ, You J, Dai Y, Shi ML, Han CP, Xu K, Anal. Chem 2014, 86, 11306. [PubMed: 25338209]

[205]. Kuo TR, Lai WY, Li CH, Wun YH, Chang HC, Chen JS, Yang P, Chen CC, Nano Res. 2014, 7, 658.

[206]. Zhou CS, Chen T, Wu CC, Zhu GZ, Qiu LP, Cui C, Hou WJ, Tan WH, Chem. Asian J 2015, 10, 166. [PubMed: 25377905]

[207]. Qiang WB, Hu HT, Sun L, Li H, Xu DK, Anal. Chem 2015, 87, 12190. [PubMed: 26556471]
[208]. Tao W, Zeng XW, Wu J, Zhu X, Yu XH, Zhang XD, Zhang JX, Liu G, Mei L, Theranostics 2016, 6, 470. [PubMed: 26941841]
[209]. Jia L, Ding L, Tian JW, Bao L, Hu YP, Ju HX, Yu JS, Nanoscale 2015, 7, 15953. [PubMed: 26367253]
[210]. Wang CH, Huang YF, Yeh CK, Langmuir 2011, 27, 6971. [PubMed: 21553884]
[211]. Fan Z, Sun LM, Huang YJ, Wang YZ, Zhang MJ, Nat. Nanotechnol 2016, 11, 388. [PubMed: 26751169]
[212]. Zhang PF, Zhao Z, Li CS, Su HF, Wu YY, Kwok RTK, Lam JWY, Gong P, Cai LT, Tang BZ, Anal. Chem 2018, 90, 1063. [PubMed: 29275625]
[213]. Zhao ZL, Fan HH, Zhou GF, Bai HR, Liang H, Wang RW, Zhang XB, Tan WH, J. Am. Chem. Soc 2014, 136, 11220. [PubMed: 25061849]
[214]. Silverman SK, RNA 2003, 9, 377. [PubMed: 12649489]
[215]. Famulok M, Hartig JS, Mayer G, Chem. Rev 2007, 107, 3715. [PubMed: 17715981]
[216]. Soukup GA, Breaker RR, Trends Biotechnol. 1999, 17, 469. [PubMed: 10557159]
[217]. Zhou ZJ, Xiao L, Xiang Y, Zhou J, Tong AJ, Anal. Chim. Acta 2015, 889, 179. [PubMed: 26343441]
[218]. Liu JW, Lu Y, Anal. Chem 2004, 76, 1627. [PubMed: 15018560]
[219]. Ayukawa S, Sakai Y, Kiga D, Chem. Commun 2012, 48, 7556.
[220]. Yang Y, Huang J, Yang X, Quan K, Wang H, Ying L, Xie N, Ou M, Wang K, Anal. Chem 2016, 88, 5981. [PubMed: 27167489]
[221]. Yang P, Wang J, Pang Q, Zhang F, Wang J, Wang Q, Qi Q, Metab. Eng 2017, 43, 21. [PubMed: 28780284]
[222]. Wieland M, Berschneider B, Erlacher MD, Hartig JS, Chem. Biol 2010, 17, 236. [PubMed: 20338515]
[223]. Ogawa A, Maeda M, Chembiochem. 2008, 9, 206. [PubMed: 18098257]
[224]. Wieland M, Hartig JS, Angew. Chem 2008, 47, 2604. [PubMed: 18270990]
[225]. Berschneider B, Wieland M, Rubini M, Hartig JS, Angew. Chem 2009, 48, 7564. [PubMed: 19739151]
[226]. Kumar D, An CI, Yokobayashi Y, J. Am. Chem. Soc 2009, 131, 13906. [PubMed: 19788322]
[227]. Win MN, Smolke CD, Science 2008, 322, 456. [PubMed: 18927397]
[228]. Ketzer P, Haas SF, Engelhardt S, Hartig JS, Nettelbeck DM, Nucleic Acids Res. 2012, 40, e167. [PubMed: 22885302]
[229]. Ketzer P, Kaufmann JK, Engelhardt S, Bossow S, von Kalle C, Hartig JS, Ungerechts G, Nettelbeck DM, Proc. Natl. Acad. Sci. USA 2014, 111, E554. [PubMed: 24449891]
[230]. Zhong G, Wang H, Bailey CC, Gao G, Farzan M, Elife 2016, 5.
[231]. Tang W, Hu JH, Liu DR, Nat. Commun 2017, 8, 15939. [PubMed: 28656978]
[232]. Wu X, Chen J, Wu M, Zhao JXJ, Theranostics 2015, 5, 322. [PubMed: 25699094]
[233]. Ying ZM, Wu Z, Tu B, Tan WH, Jiang JH, J. Am. Chem. Soc 2017, 139, 9779. [PubMed: 28714696]
[234]. Lu DQ, He L, Zhang G, Lv AP, Wang RW, Zhang XB, Tan WH, Nanophotonics 2017, 6, 109.

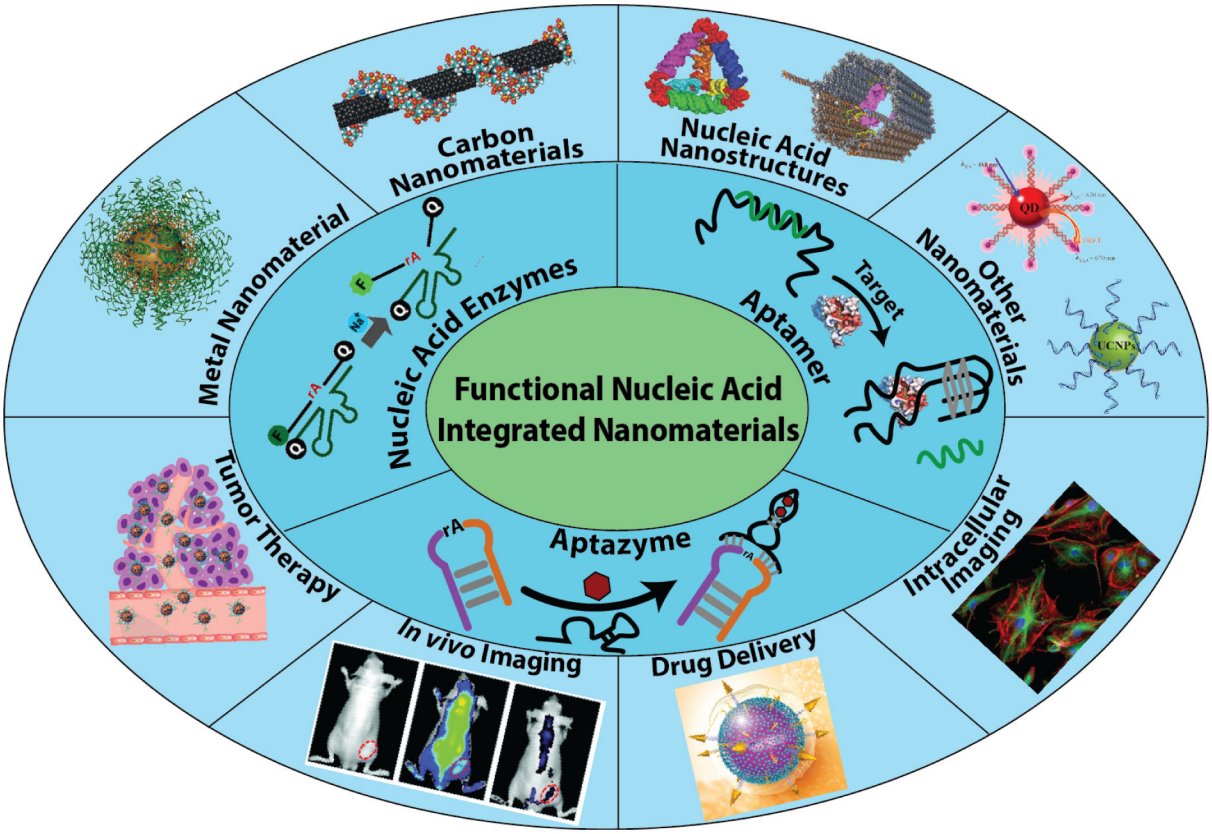

Figure 1.

The schematic illustration of functional nucleic acid integrated nanomaterials toward diverse biomedical applications.

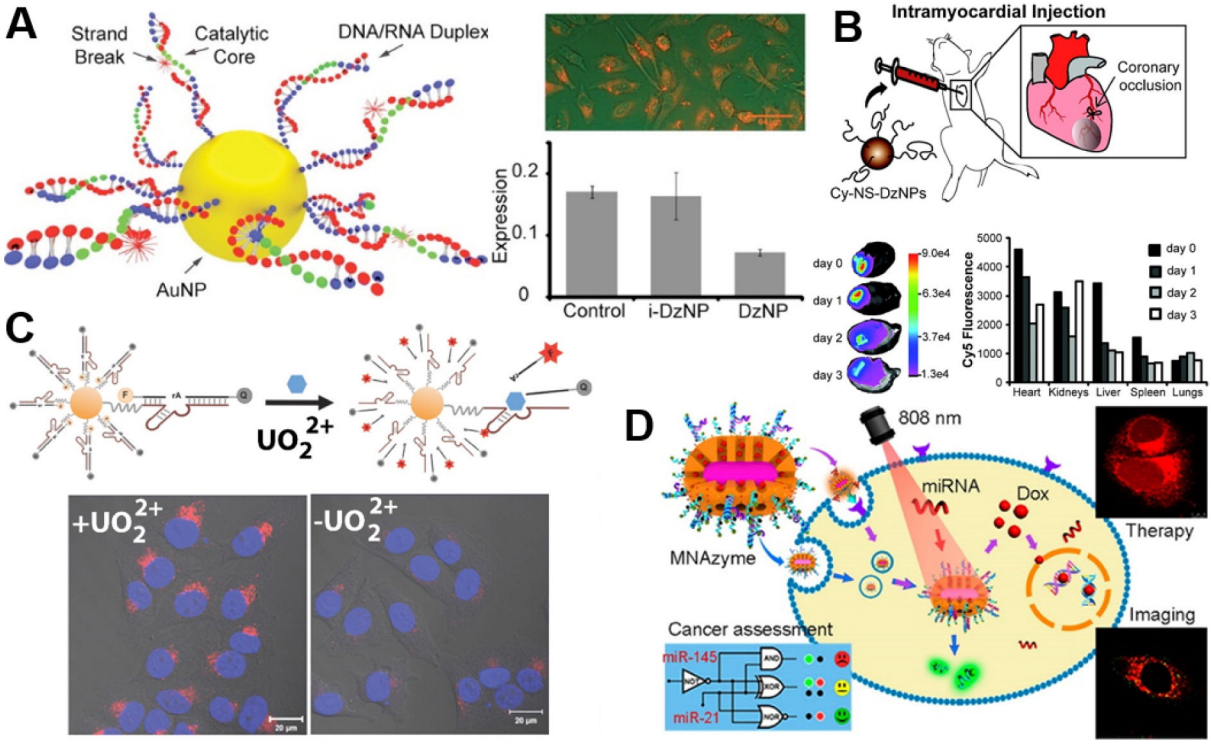

Figure 2.

Integration of nucleic acid enzymes with noble metal nanomaterials toward *in vivo* applications. A) Catalytic deoxyribozyme-modified gold nanoparticles for RNAi-independent gene regulation. Reproduced with permission.[18] Copyright 2012, American Chemical Society. B) Ex-vivo fluorescence imaging of organs from animals injected with DNAzyme gold nanoparticles as an anti-inflammatory therapy via TNF-α knockdown. Reproduced with permission. [19] Copyright 2016, Elsevier. C) Fluorescent imaging of intracellular uranyl based on gold nanoparticles-DNAzyme probe. Reproduced with permission. [21] Copyright 2013, American Chemical Society. D) Schematic illustration of the multicomponent nucleic acid enzymes (MNAzymes) integrated gold nanorods for intracellular miRNA imaging, controlled drug release and therapy. Reproduced with permission. [27] Copyright 2015, American Chemical Society.

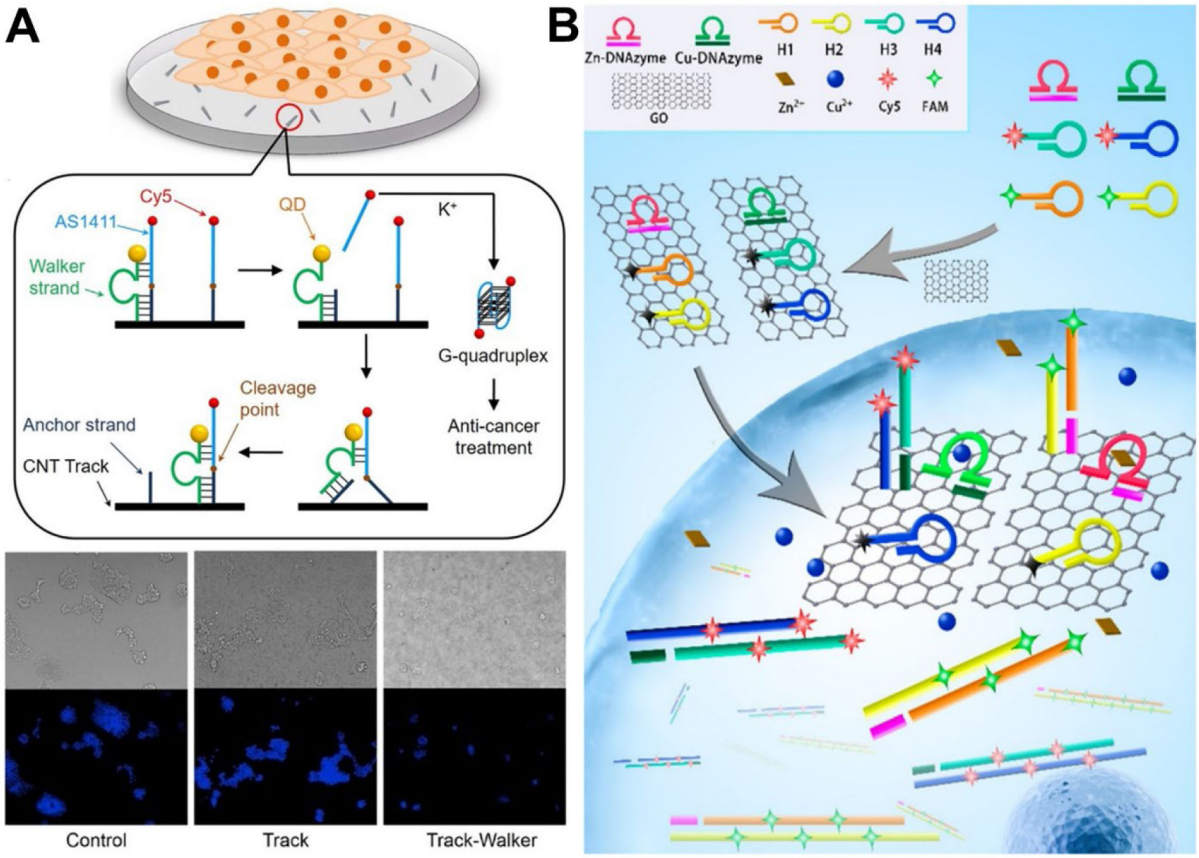

Figure 3.

A) DNA walker-mediated platform for inhibiting cancer cell growth. Top: Walking mechanism. Bottom: Bright-field and fluorescence images of MCF-7 cells on collagen extracellular matrix after 120 h of culture. Reproduced with permission. [32] Copyright 2016, Wiley-VCH. B) Fluorescence imaging of Zn^{2+} and Cu^{2+} in living cells using DNAzymes-integrated graphene oxide nanosheets. Reproduced with permission. [33] Copyright 2018, American Chemical Society.

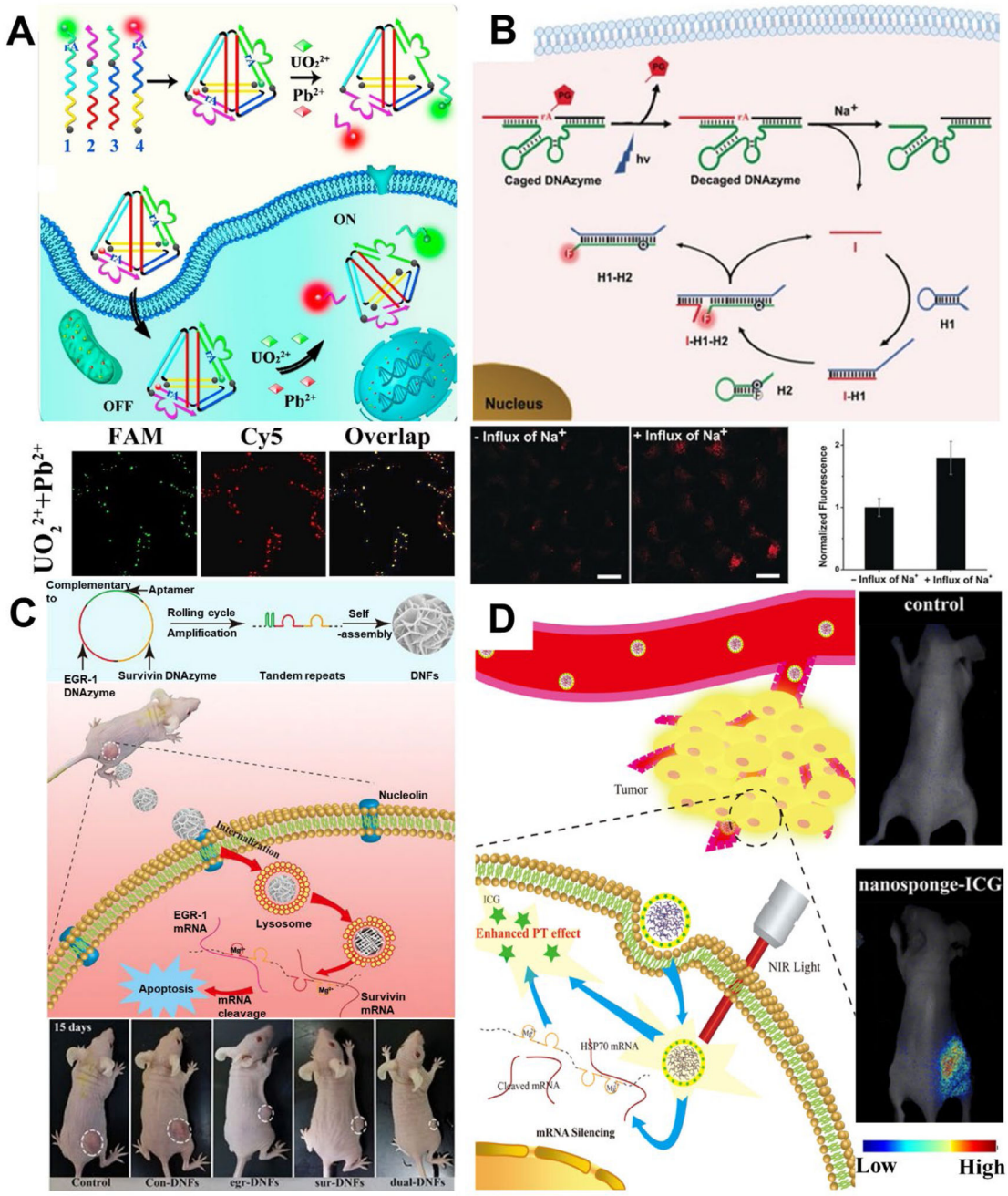

Figure 4.

A) Multiplexed fluorescent imaging of intracellular UO_2^{2+} and Pb^{2+} with the DNAzyme integrated tetrahedron nanoprobes. Reproduced with permission.[36] Copyright 2016, Elsevier. B) DNAzyme-catalytic hairpin assembly probe for fluorescent imaging of endogenous sodium ion in living cells. Reproduced with permission.[37] Copyright 2017, Wiley-VCH. C) Illustration of the self-assembly of DNAzyme nanoflowers, and the applications for mRNA silencing and tumor inhibition. Reproduced with permission.[39] Copyright 2017, Nature Publishing Group. D) Illustration of DNAzyme-based nanosponges

for highly efficient photothermal therapy. Reproduced with permission.[41] Copyright 2018, Nature Publishing Group.

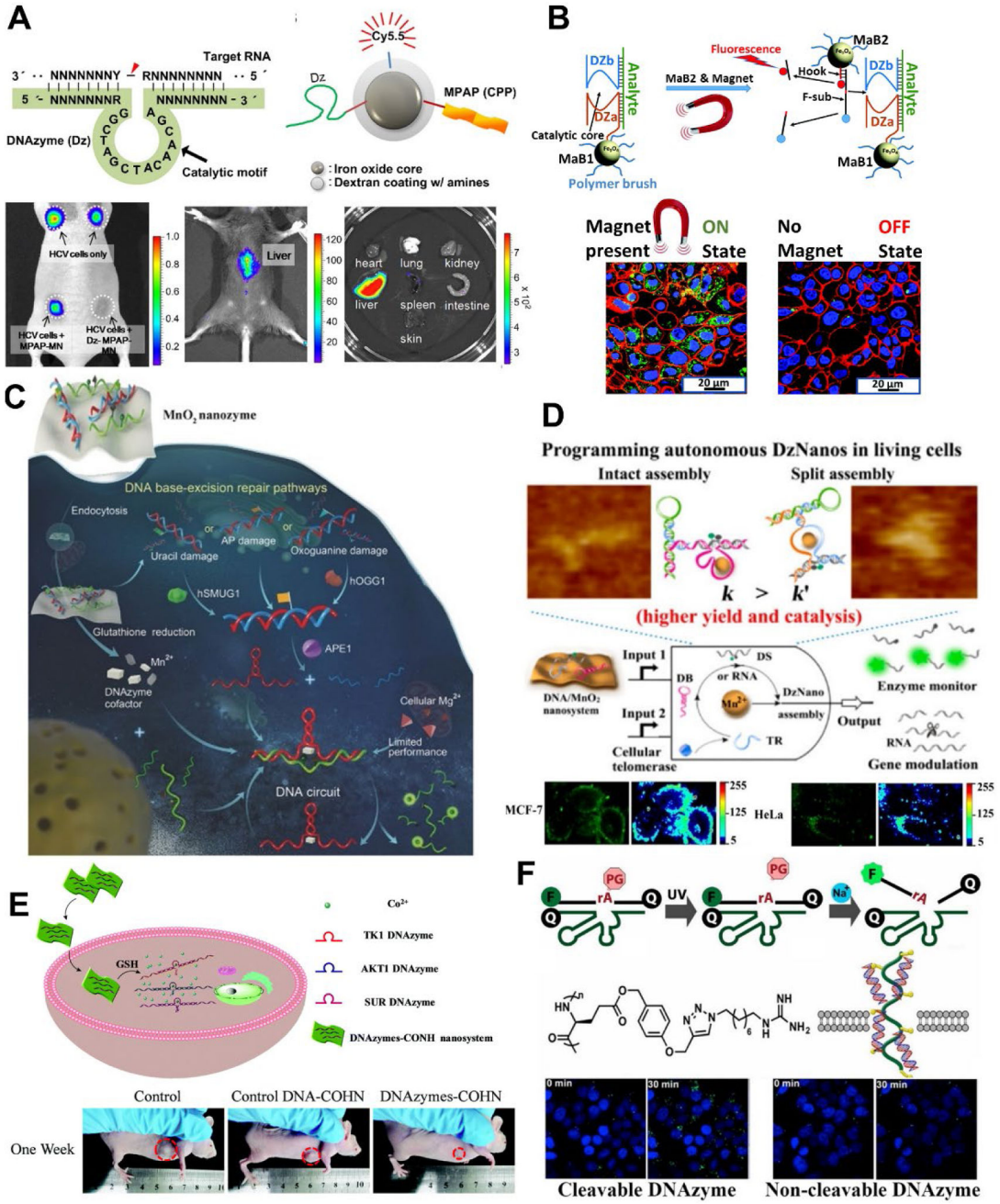

Figure 5.

A) Multifunctional iron oxide nanoparticle formulation for 10–23 DNAzyme delivery for hepatitis C virus gene knockdown. Bottom: in vivo biodistribution. Reproduced with permission.[43] Copyright 2012, Elsevier. B) Magnetic field-activated deoxyribozyme nanoreactor for imaging of MCF-7 cells. Reproduced with permission.[44] Copyright 2018, The Royal Society of Chemistry. C) Illustration of intracellular MnO_2 nanozyme-catalyzed DNA circuit for versatile monitoring of DNA base-excision repair pathways in living cells. Reproduced with permission.[46] Copyright 2017, Wiley-VCH. D) Programming telomerase-initiated autonomous DNAzyme nanodevices in living cells to monitor enzyme catalysis *in*

situ and gene regulation. Reproduced with permission.[47] Copyright 2017, American Chemical Society. E) Schematic illustration of DNAzymes–CONH nanocomposite for gene silencing. Reproduced with permission.[48] Copyright 2017, The Royal Society of Chemistry. F) Intracellular imaging of sodium ions based on cationic polypeptides and photocaged Na^+-DNAzyme. Reproduced with permission.[52] Copyright 2015, PNAS.

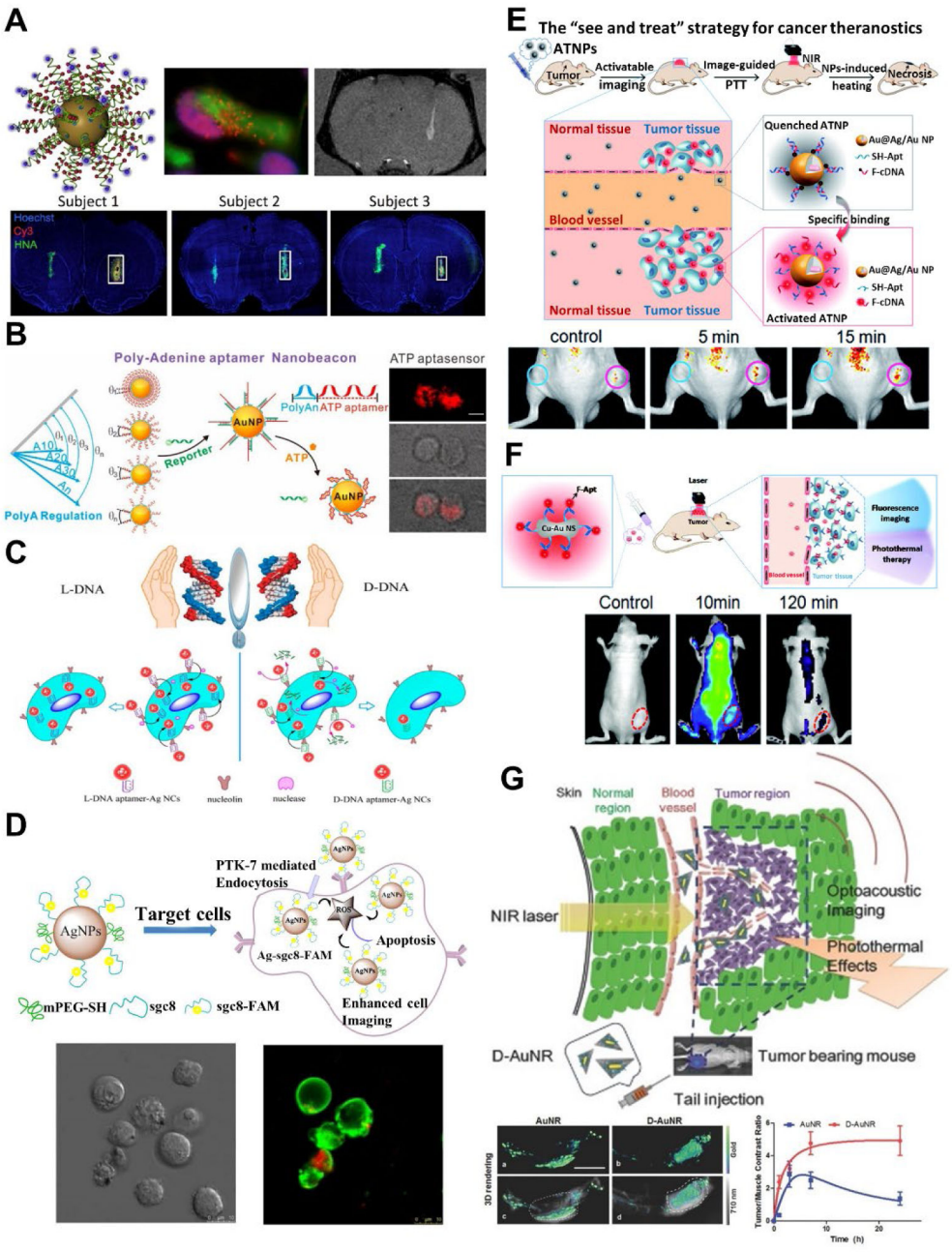

Figure 6.

A) DNA-gadolinium-gold nanoparticles for *in vivo* T1 MRI of transplanted human neural stem cells. Reproduced with permission.[66] Copyright 2016, Elsevier. B) PolyA-based engineered aptamer-gold nanoparticles nanobeacon for intracellular ATP imaging. Reproduced with permission.[68] Copyright 2017, American Chemical Society. C) Biostable L-DNA-templated aptamer-silver nanoclusters for targeted imaging. Reproduced with permission.[83] Copyright 2016, American Chemical Society. D) Multifunctional aptamer −silver conjugates as theragnostic agents for specific cancer cell therapy and fluorescence-enhanced cell imaging. Reproduced with permission.[86] Copyright 2015, American

Chemical Society. E) Scheme of the activatable aptamer-integrated Au@Ag/Au nanoparticles for *in vivo* cancer imaging and the guided photothermal therapy. Reproduced with permission.[88] Copyright 2014, The Royal Society of Chemistry. F) The fluorophore-labeled aptamer/Cu–Au nanostructure and its application for *in vivo* fluorescence tumor imaging and NIR photothermal therapy. Reproduced with permission.[89] Copyright 2016, The Royal Society of Chemistry. G) NA-origami–gold-nanorod hybrid nanosystem for enhanced *in vivo* optoacoustic imaging and photothermal therapy. Reproduced with permission. [92] Copyright 2016, Wiley-VCH.

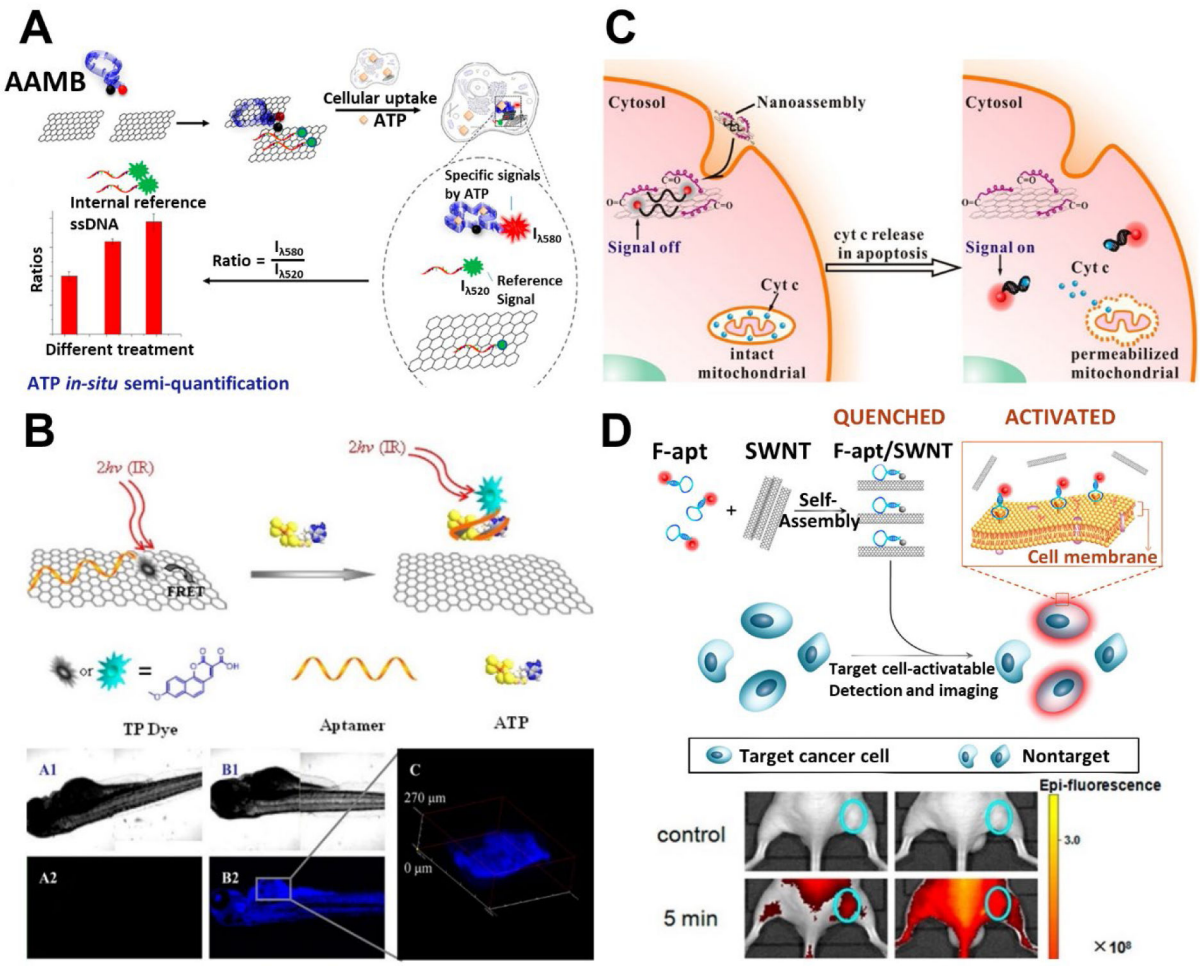

Figure 7.

A) Semiquantification of ATP in live cells using aptamer modified graphene oxide. Reproduced with permission.[97] Copyright 2012, American Chemical Society. B) Illustration of two-photon graphene oxide/aptamer-based nanosensing conjugate for ATP probing in Zebrafish. Reproduced with permission.[100] Copyright 2014, American Chemical Society. C) fluorescence activation imaging of Cytochrome c released from mitochondria using aptamergraphene oxide nanoprobes. Reproduced with permission.[103] Copyright 2015, American Chemical Society. D) Schematic representation of the novel activatable fluorescence probing strategy for target cancer cells based on self-assembled fluorophore-labeled aptamer/single-walled carbon nanotube ensembles. Reproduced with permission.[105] Copyright 2014, American Chemical Society.

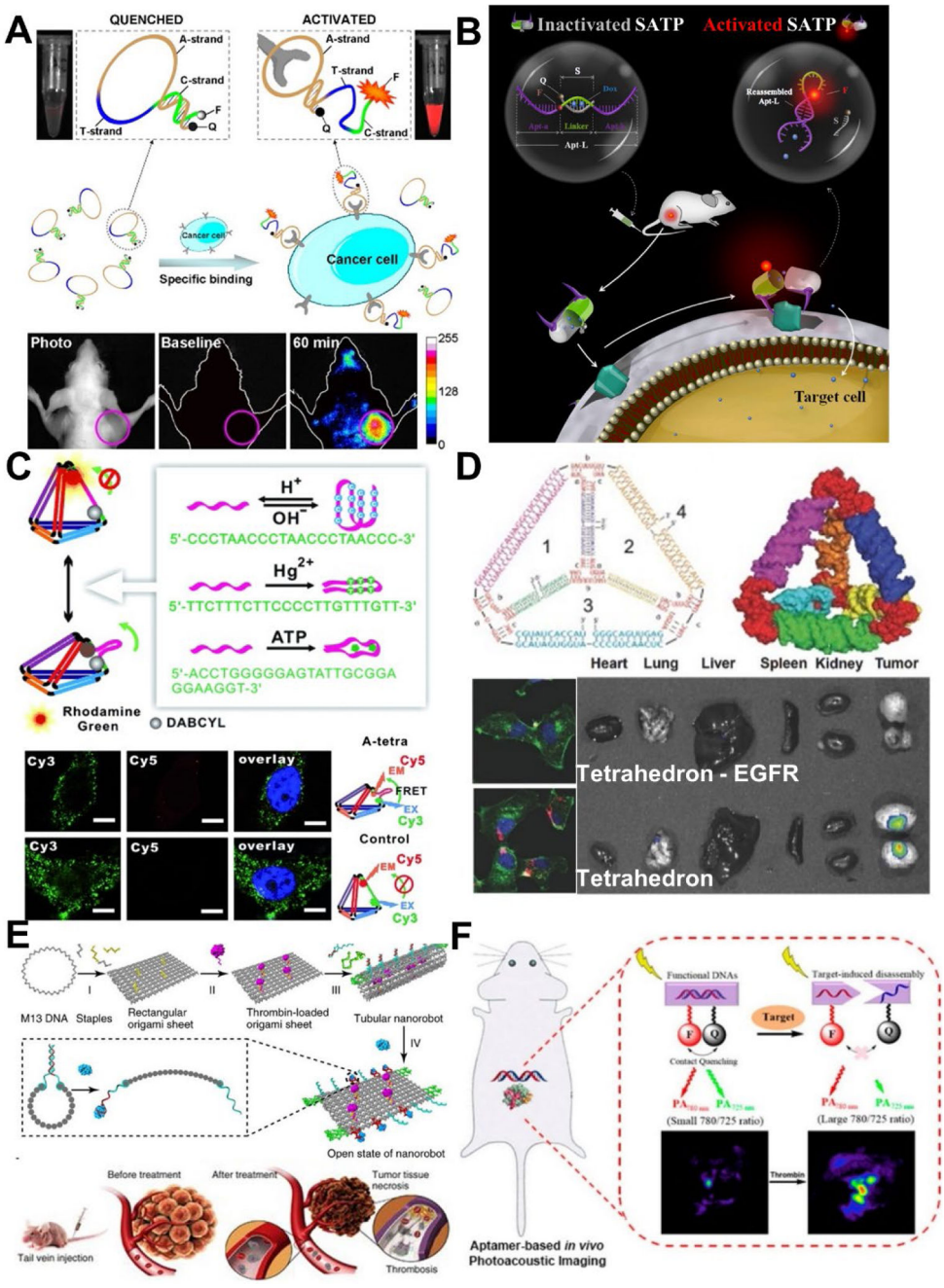

Figure 8.

A) Activatable aptamer probe for *in vivo* cancer imaging based on cell membrane protein-triggered conformation alteration. Reproduced with permission.[109] Copyright 2011, PNAS. B) Split aptamer-based activatable theranostic probe (SATP) for *in vivo* cancer imaging. Reproduced with permission.[111] Copyright 2016, American Chemical Society. C) Aptamer-embedded DNA tetrahedral nanostructures for intracellular logic sensors. Reproduced with permission.[116] Copyright 2012, Wiley-VCH. D) Aptamer-embedded RNA tetrahedral nanostructures for cancer targeting. Reproduced with permission.[119] Copyright 2016, Wiley-VCH. E) Illustration of the construction of thrombin-loaded

nanorobot by aptamer-embedded DNA origami as a cancer therapeutic. Reproduced with permission.[129] Copyright 2018, Nature Publishing Group. F) Aptamer-based DNA nanoprobes for *in vivo* photoacoustic imaging. Reproduced with permission.[135] Copyright 2017, American Chemical Society.

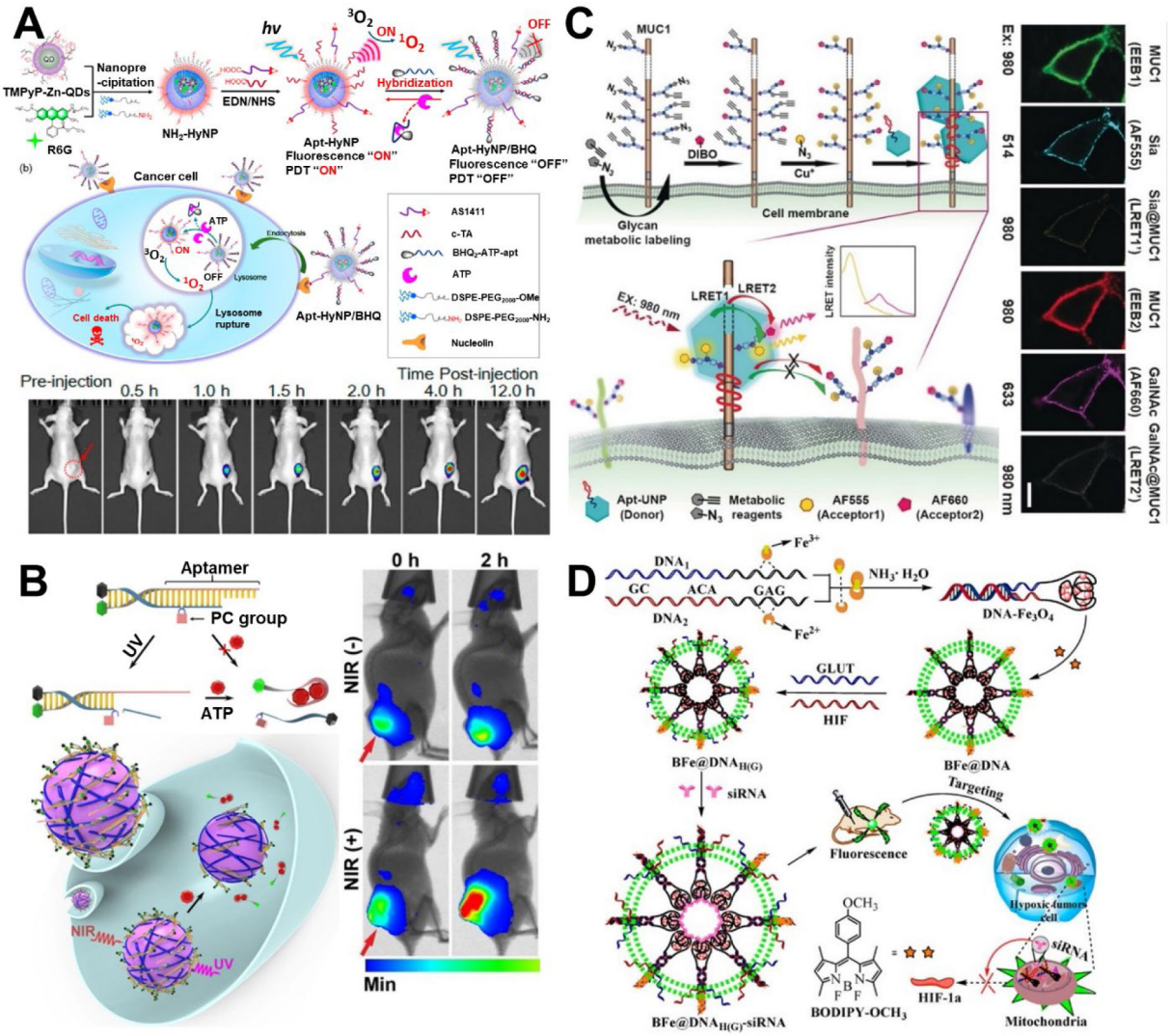

Figure 9.

A) General design of tumor-targeting and ATP-activatable photosensitizer for fluorescence imaging and PDT of tumors. Reproduced with permission.[149] Copyright 2017, American Chemical Society. B) NIR-activatable DNA nanodevices for *in vivo* ATP imaging based on the integration of the aptamer probe with upconversion nanotransducer. Reproduced with permission.[155] Copyright 2018, American Chemical Society. C) The site-specific DLRET method for duplexed imaging and dynamic monitoring of protein-specific monosaccharides on an intact cell surface based on aptamer-functionalized upconversion nanoparticles. Reproduced with permission.[161] Copyright 2016, Wiley-VCH. D) The assembly of functional magnetic nanoaptamer for cancer gene therapy. Reproduced with permission.[173] Copyright 2018, American Chemical Society.

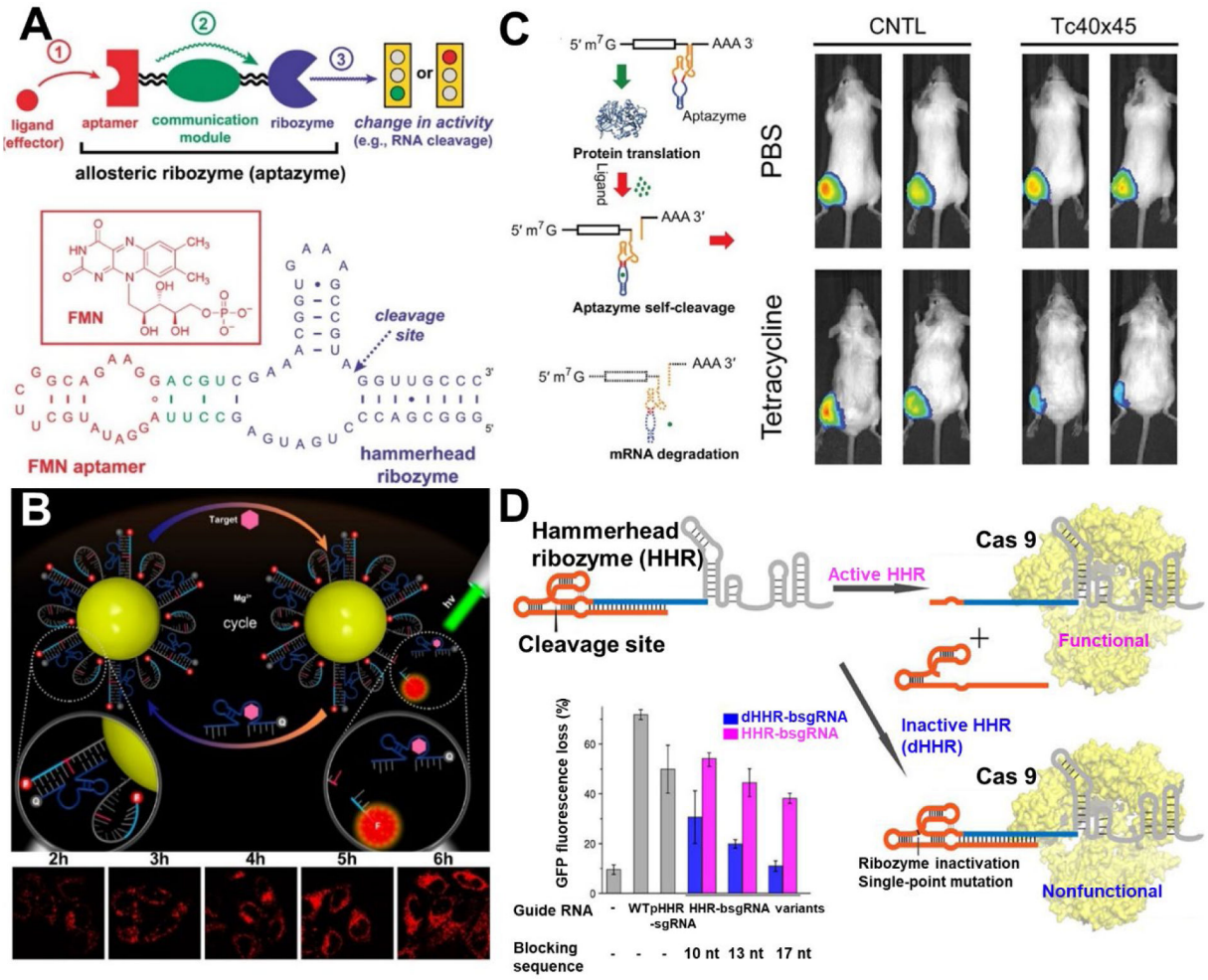

Figure 10.

A) General strategy for creation of an allosteric ribozyme (aptazyme), depicting the aptamer, communication, and ribozyme modules. Bottom: an allosteric ribozyme for flavin mononucleotide. Reproduced with permission.[214] Copyright 2003, CSH Press. B) Gold nanoparticles based aptazyme for intracellular ATP imaging. Reproduced with permission.[220] Copyright 2016, American Chemical Society. C) Rational design of aptazyme riboswitches for efficient control of gene expression in mammalian cells. Reproduced with permission.[230] Copyright 2016, Howard Hughes Medical Institute. D) Aptazyme-embedded guide RNAs for ligand-responsive genome editing and transcriptional activation. Reproduced with permission.[231] Copyright 2017, Nature Publishing Group.

Table 1.

A list of representative NAEs integrated with other nanomaterials toward *in vivo* applications

Types of Nanomaterials	Type of NAEs	Analyte	Applications	Ref.
Iron oxide	10–23 10–23	hepatitis C gene DNA or RNA	*In vivo* treatment of hepatitis C Intracellular bioimaging and biocatalysis	[43] [44]
MnO_2 nanosheets	$Mn2^+$-dependent $Mn2^+$-dependent $Mn2^+$-dependent	RNA Endonuclease and glycosylase Telomerase	Gene silencing and photodynamic therapy Intracellular monitoring of DNA base-excision repair pathway Intracellular monitoring of enzyme catalysis	[45] [46] [47]
CoOOH nanosheets	Co^{2+}-dependent	RNA	Intracellular and *in vivo* gene silencing	[48]
Dendritic polymer	Pb^{2+}-dependent	Pb^{2+}	Intracellular imaging of Pb^{2+}	[49]
MOFs	Zn^{2+}-DNAzyme	miRNA-21	Intracellular imaging of miRNA	[50]
UCNPs	Zn^{2+}-dependent	Zn^{2+}	Intracellular and in vivo imaging of Zn^{2+}	[51]
Cationic polypeptides	Na^+-dependent	Na^+	Intracellular imaging of Na^+	[52]

Table 2.

A list of representative aptamers integrated with other nanomaterials toward *in vivo* applications

Types of nanomaterials	Aptamer targeting molecues	Applications	Ref.
QDs	Mucin 1	Targeted cell imaging and sensing	[146–148]
	Nucleolin and ATP	Imaging-guided tumor therapy	[149]
UCNPs	ATP	Intracellular and *in vivo* sensing	[155]
	Nucleolin	Targeted cell imaging	[157, 158]
	PTK7	Imaging-guided tumor therapy	[159]
	Mucin 1	Profile cell surface glycoforms	[161]
MNPs	Adenosine	MRI detection of secreted enzyme	[167]
	HL-60 cells	Targeted cell imaging	[168]
	Mucin 1	Targeted cancer therapy	[173, 174]
Liposome	Nucleolin	Cell-specific drug delivery	[182, 183]
	EGF receptor	siRNA delivery and imaging	[186]
Silica nanomaterials	Nucleolin	Cell and *in vivo* imaging	[187–190]
	MUC-1	Cancer cell detection	[191, 192]
	PTK7	Cell-specific drug delivery	[193]
	Mouse endoglin	Targeted cancer therapy	[194]
Polymer nanomaterials	PSMA	Targeted cell imaging	[195]
	Nucleolin	In vivo glioma imaging and therapy	[196, 197]
	EpCAM	Switchable cell imaging	[198]
MOFs	ATP	Intracellular ATP imaging	[199]
Dendrimers	Nucleolin	*In vivo* cancer theranostics	[200]
	Endoglin	*In vivo* multimodal tumor imaging	[201]
Micellar	MDA-MB-231	Targeted cancer therapy	[202]
	Nucleolin	NIR cancer therapy	[203]
Gadolinium oxide	Nucleolin	Targeted cell imaging	[204, 205]
$CaCO_3$	PTK7	Drug delivery and imaging	[206]
Polydopamine	Nucleolin	Targeted cancer therapy	[207, 208]
MoS_2 nanoplates	ATP	Intracellular ATP imaging and PDT	[209]
Lipid nanobubbles	PTK7	Targeted ultrasound cell imaging	[210]
AIE organic dots	Nucleolin	Targeted cell imaging	[212]
MnO_2 nanosheet	PTK7	Bimodal tumor imaging	[213]